REPORT DOCUMENTATION PAGE

Form Approved
OMB No. 0704-0188

1. AGENCY USE ONLY (Leave blank)	2. REPORT DATE	3. REPORT TYPE AND DATES COVERED
	12 Apr 96	Final 15 Jul 95 - 14 Jan 96

4. TITLE AND SUBTITLE
Advanced Processing of Nonlinear Optical Materials to Lower Pigtailing Cost, Reduce Optical Loss, and Reduce Drive Voltages in Devices

5. FUNDING NUMBERS
C - F49620-95-C-0053
1660/01
62173C

6. AUTHOR(S)
Robert V. Mustacich

7. PERFORMING ORGANIZATION NAME(S) AND ADDRESS(ES)
RVM Scientific, Inc.
722 Camino Cascada
Santa Barbara, CA 93111-1403

8. PERFORMING ORGANIZATION REPORT NUMBER
RVMS-CR-96-01

9. SPONSORING/MONITORING AGENCY NAME(S) AND ADDRESS(ES)
Air Force Office of Scientific Research/NL
110 Duncan Avenue, Suite B115
Bolling AFB DC 20332-0001
Dr Lee

10. SPONSORING/MONITORING AGENCY REPORT NUMBER
AFOSR-TR-96
0180

11. SUPPLEMENTARY NOTES

12a. DISTRIBUTION/AVAILABILITY STATEMENT
Approved for public release;
distribution unlimited.

12b. DISTRIBUTION CODE

13. ABSTRACT *(Maximum 200 words)*

The feasibility investigation of advanced photoprocessing using multicolor lithography with NLO polymers is presented. Photoprocessing has previously been demonstrated using ultraviolet bleaching of NLO polymer films to define waveguides and gratings. This processing approach presented in this report is the first investigation of using the wavelength dependence of photoprocessing to control refractive index gradients in NLO polymer films. This approach makes possible for the first time the 3-dimensional control of refractive index gradients within NLO polymer films to fabricate advanced waveguide structures such as buried waveguides and vertical tapers. This fabrication method offers unique potential for low optical losses by substituting optically defined graded index boundaries for mechanically created boundaries in channel waveguides. This processing approach also offers great simplicity in fabrication to boost productivity and lower fabrication cost. Most importantly, multicolor lithography of NLO polymers can provide a unique route to achieving NLO polymer devices having low insertion losses and low drive voltages through 3-D waveguide fabrications made possible by this approach.

14. SUBJECT TERMS		15. NUMBER OF PAGES
Insertion Loss	Optical Waveguides	41
NLO Polymer Materials	Electro-Optic Devices	16. PRICE CODE

17. SECURITY CLASSIFICATION OF REPORT	18. SECURITY CLASSIFICATION OF THIS PAGE	19. SECURITY CLASSIFICATION OF ABSTRACT	20. LIMITATION OF ABSTRACT
UNCLASSIFIED	UNCLASSIFIED	UNCLASSIFIED	

DISCLAIMER NOTICE

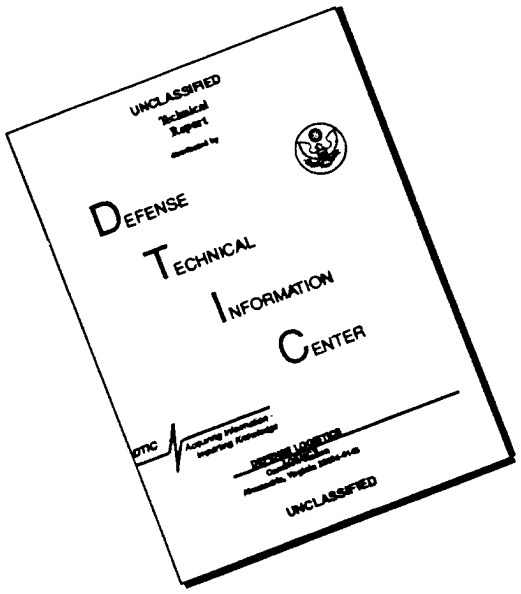

THIS DOCUMENT IS BEST QUALITY AVAILABLE. THE COPY FURNISHED TO DTIC CONTAINED A SIGNIFICANT NUMBER OF PAGES WHICH DO NOT REPRODUCE LEGIBLY.

TABLE OF CONTENTS

Section

1.0 SUMMARY

The feasibility investigation of advanced photoprocessing using multicolor lithography with NLO polymers is presented. Photoprocessing has previously been demonstrated using ultraviolet bleaching of NLO polymer films to define waveguides and gratings. This processing approach presented in this report is the first investigation of using the wavelength dependence of photoprocessing to control refractive index gradients in NLO polymer films. This approach makes possible for the first time the 3-dimensional control of refractive index gradients within NLO polymer films to fabricate advanced waveguide structures such as buried waveguides and vertical tapers. This fabrication method offers unique potential for low optical losses by substituting optically defined graded index boundaries for mechanically created boundaries in channel waveguides. This processing approach also offers great simplicity in fabrication to boost productivity and lower fabrication cost. Most importantly, multicolor lithography of NLO polymers can provide a unique route to achieving NLO polymer devices having low insertion losses and low drive voltages through 3-D waveguide fabrications made possible by this approach. The technology feasibility demonstrations and these applications are discussed at length in this report.

2.0 INTRODUCTION

Fiber optics offers transmission of data without repeaters and has an enormous bandwidth potential. Ultra fast optical modulation using nonlinear optical (NLO) polymers is technology which will enable optical computing, optical signal processing and the huge bandwidth potential of fiber telecommunications and chip-to-chip interconnections to be realized. In particular, NLO polymers provide materials with the processing flexibility required to create waveguides with strong electro-optic (EO) response to join other materials such as silicon or gallium arsenide semiconductors into hybrid integrated optical circuits. Current NLO polymers have been used to demonstrate approaches to meeting the requirements for NLO polymer-based devices and chip-to-chip interconnects, *but these demonstrated approaches usually address only a single requirement at a time.* These requirements include: NLO polymers containing chromophores having large hyperpolarizabilities which can provide thermally stable, strong EO response; NLO polymer and polymer device compatibility and stability with standard manufacturing processes for integrated circuits and chip bonding; fabrication processes with fine control of low loss buried waveguides and low cost, robust pigtailing; and effective integration of large bandwidth drive electrodes with silicon or gallium arsenide semiconductors to achieve low drive voltages.

While large increases in thermal stability have been achieved with higher melting temperature polymer matrices and crosslinking, the steps taken typically reduce the effective EO response of NLO polymers. Further, sophisticated waveguide processing and the other fabrication requirements for a practical device have not been demonstrated in a unified approach, i.e., low optical losses demonstrated without coupling to fibers, or efficient fiber coupling demonstrated without fabricating modulator electrodes, etc. RVM Scientific (RVMS) has been working to develop fabrication approaches which combine new NLO polymers which are intrinsically thermodynamically stable with innovative processing. This research was conducted with the subcontracting support of one of the leading laboratories (Dr. Larry Dalton, University of Southern California (USC)) in the field of thermally-stable, latticed-hardened NLO polymers.

This research aims to solve an important processing challenge for the formation of optical waveguides in optical polymer films which interface well with optical fibers, have very low propagation losses, and have low loss transitions to waveguides of small dimensions for reducing drive voltages. While a number of approaches have been used for processing waveguides in these materials, there are trade-offs between mode size, single mode support, refractive index gradients, mode penetration of the cladding and resulting losses, and accompanying processing problems such as residual stresses in three-layer film devices. Resulting mode size and shape mismatches in going from fiber to thin film devices and back to fiber are illustrated in Figure 1. The large mode size of a single mode fiber is shown on the left. If a sufficiently thick NLO polymer film is used to fabricate an EO waveguide (shown top center) with a mode size to match the fiber, this waveguide will not be single mode unless the refractive indices of at least one of the claddings is near that of the NLO polymer. For most organic polymers, finding a suitable cladding would not be a problem, but NLO polymers have large indices compared to most materials. For a several micron waveguide to be single mode at optical frequencies, it is further necessary for the mode to evanesce somewhat into the cladding. This is a consequence of the small Δn difference with the cladding which prevents higher order modes from waveguiding (i.e., higher order modes fully leak into the cladding while the lowest order mode does not). Accordingly, thick claddings are illustrated in Figure 1. Thick NLO polymers and cladding films result in a large spacing of electrodes outside the cladding layers. This unfortunately reduces the effective electric field in the NLO polymer for a given applied voltage.

The bottom center of Figure 1 shows a more ideal electrode spacing in which claddings with a larger Δn provide single mode waveguiding in a thinner NLO film. This smaller electrode spacing greatly increases the effective electric field for a given drive voltage. Such thin films are typical of single mode waveguides using NLO polymers with ordinary cladding materials. However, as graphically suggested in the figure, smaller waveguides will have a large size mismatch when attempting to couple NLO polymer waveguides to single mode optical fiber. This mismatch can result in insertion losses upwards of 10 dB for small waveguides. Note also, though, that smaller cladding thicknesses are typically required owing to the reduced mode penetration of the larger Δn claddings.

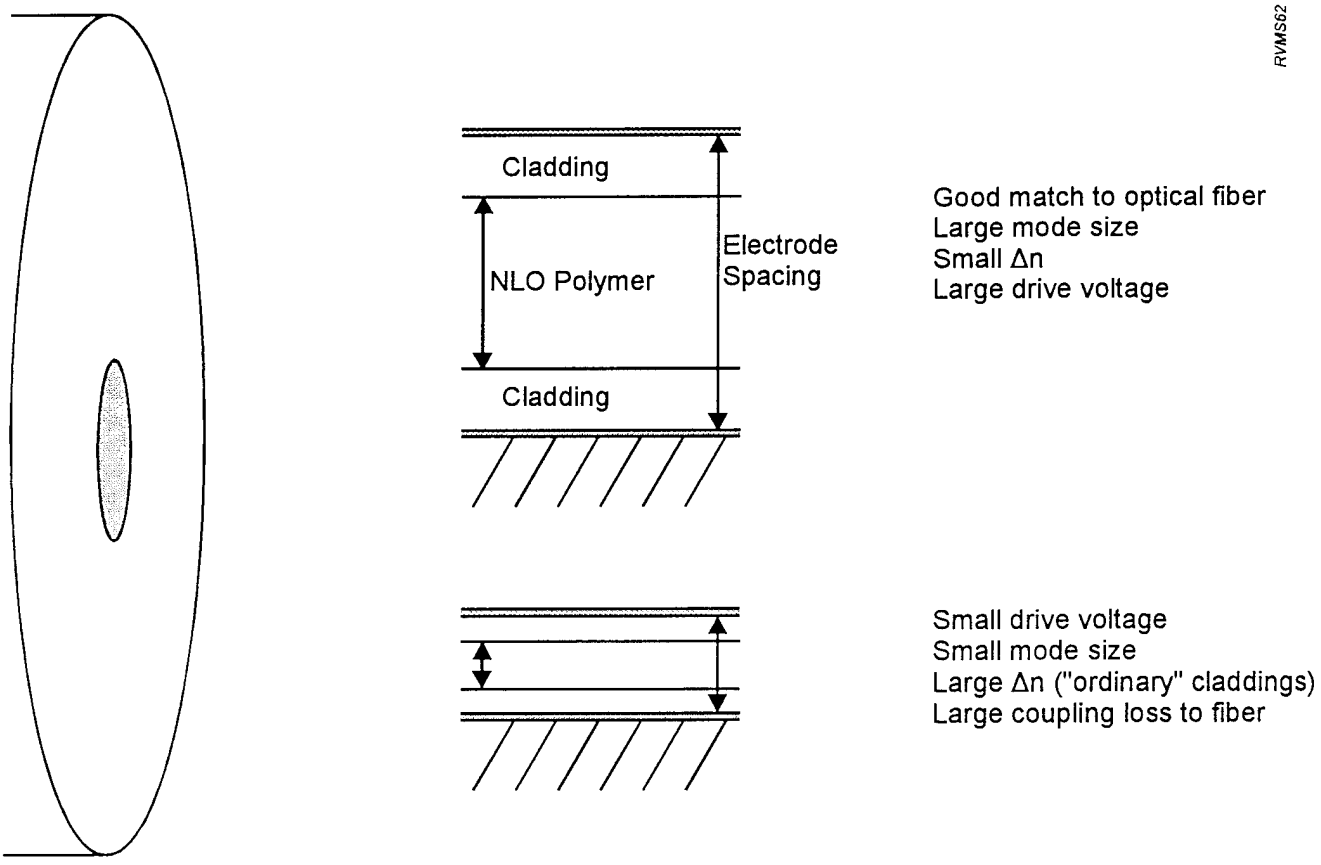

Figure 1. Graphical illustration of trade-offs between matching mode sizes of single mode fiber for low insertion loss and realizing small drive voltages.

This discussion regarding Figure 1 describes the tradeoff between optical losses and drive voltage in seeking a waveguide which couples well to fibers, but is also intended to provide efficient EO modulation. Using specialized low Δn claddings that were polymer blends of the NLO core layer, we have previously fabricated waveguides for polymer phase modulators only to find that these trade-offs resulted in serious compromises of optical insertion loss and drive voltage (Mustacich et al., 1992). NLO polymers were successfully taken to their limiting linear EO (r) coefficients, but both losses and drive voltages were unacceptable. Fiber coupling losses were reduced to an acceptable 1 dB/end face, but the large mode size increased the electrode spacing. To reduce the drive voltage to more acceptable levels, the optical waveguide propagation loss was increased by reducing the cladding thickness to allow a closer electrode spacing. The measured channel waveguide propagation loss could be fully accounted for by the absorption by the electrodes of evanescent light in the cladding layer (Mustacich et al., 1992). This undesirable compromise exemplifies this fundamental trade-off in attempting to satisfy matching to the large modes of single mode fiber and fabricating small EO waveguides.

The research described in this report describes the SBIR Phase I progress on an innovative processing approach which can eliminate this trade-off in device fabrications as well as greatly simplify the fabrication of NLO polymer devices. This approach uses a new photoprocessing method to control refractive index gradients (Δn) within polymer films. This approach can replace all of the waveguide fabrication steps requiring dielectric etching with optical-only processing of a single film. Further, one or both cladding layers are eliminated by optical processing of the NLO polymer film. Through uniquely possible manipulation of the optical photoprocessing wavelength, structures such as 3-D refractive index gradients which define waveguides, waveguide tapers and branches can be made.

Applications of this new photoprocessing approach to solving the small EO waveguide-large single mode fiber matching trade-off are shown in Figure 2. In this figure a high speed semiconductor device is integrated with an NLO polymer waveguide. The photoprocessing is used to define large single mode waveguides at the fiber interface so that the optical coupling loss is small ($<<$ 1 dB). This same processing is varied along the length of the waveguide to create a transition to a small, buried waveguide. This transition consists of a vertical taper to a waveguide near the bottom of the fiber surface. Past this transition, the upper region of the NLO film can be etched to leave only a small distance separating the

electrodes. Our calculations indicate that a 2-3 μm electrode spacing with low optical waveguide propagation loss can be fabricated using this technique. This can improve current V_π values by a factor of 4-5. These waveguide tapers are then reversed to efficiently transition back to optical fiber.

This research report describes this new processing approach, its feasibility analysis, experiments conducted to demonstrate its applicability to NLO polymers, and recommended applications to NLO devices.

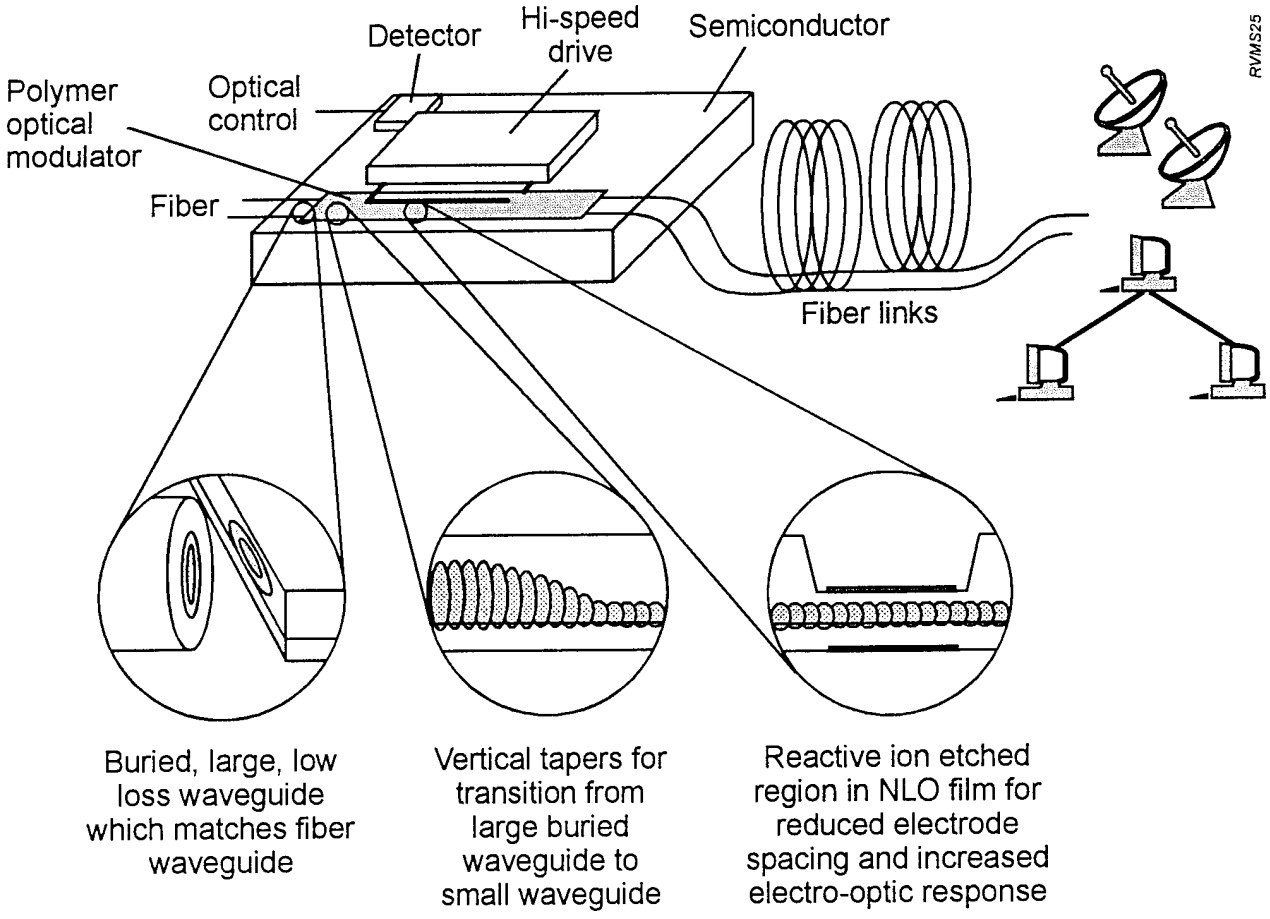

Figure 2. NLO polymer waveguide structures uniquely possible through advanced photoprocessing.

3.0 FEASIBILITY OF ADVANCED PHOTOPROCESSING OF MICROSCOPIC STRUCTURES IN NONLINEAR OPTICAL (NLO) POLYMERS

3.1 PREVIOUS PHOTOPROCESSING RESEARCH WITH ADVANCED NLO POLYMERS

The discovery of stable photoinduced changes in the refractive index of disperse red 19 (DR19)-containing NLO polymers resulting from UV light exposure led to demonstrations by USC of micro patterning of these NLO thin films using conventional lithographic methods (Shi et al., 1991; Steier et al., 1992). Examples include the fabrication of 3 to 10 μm channel waveguides in copolyester DR19 films following an exposure in a mask aligner (Shi et al., 1991), as well as thin film waveplates and birefringent diffraction gratings (Steier et al., 1992). In particular, the magnitude of the photoinduced birefringence is 2~3 orders of magnitude larger than those reported in earlier studies of dye doped polymer systems (Todorov et al., 1985; Luckemeyer and Franke, 1988). This ensures sufficiently large dynamic range for the effect that various approaches to controlling and attenuating the exposures can result in meaningful gradients for photoprocessed structures. Also important, the photoinduced refractive index changes were found to be stable over a period of 5 months (Shi et al., 1991). The long term stability of the effect is believed due to the limited mobility of the azo dye groups when the polymer temperature is well below its glass transition temperature (~120 °C for polyester DR19) and the azo groups are covalently linked to the polymer backbone. The stability is further increased by photo crosslinking of cinnamic groups in the NLO polymer backbone. This further reduces the mobility of the side groups and improves the stability.

For demonstrating the feasibility of this new photoprocessing approach described in this report, the polymer polyurethane disperse red 19 (PUDR19) was used (Chen et al., 1991). The DR19 chromophore and its photoisomerization are shown in Figure 3. The chromophore exhibits a strong absorption in the visible at 475 nm as well as in the UV and is transparent above 640 nm. The trans isomer has a lower energy and comprises the DR19 in the synthesized PUDR19. Excitation of the DR19 can result in photoisomerization as depicted in Figure 3 as well as other photoinduced reactions such as cross-linking to the polymer. The loss of the trans isomer results in a decrease of the 475 nm absorption band and a corresponding drop in refractive index proportional to the loss of the trans isomer. Photoisomerization of the chromophore in PUDR19 with UV results in a large Δn change of approximately -0.3 (Chen et al., 1991).

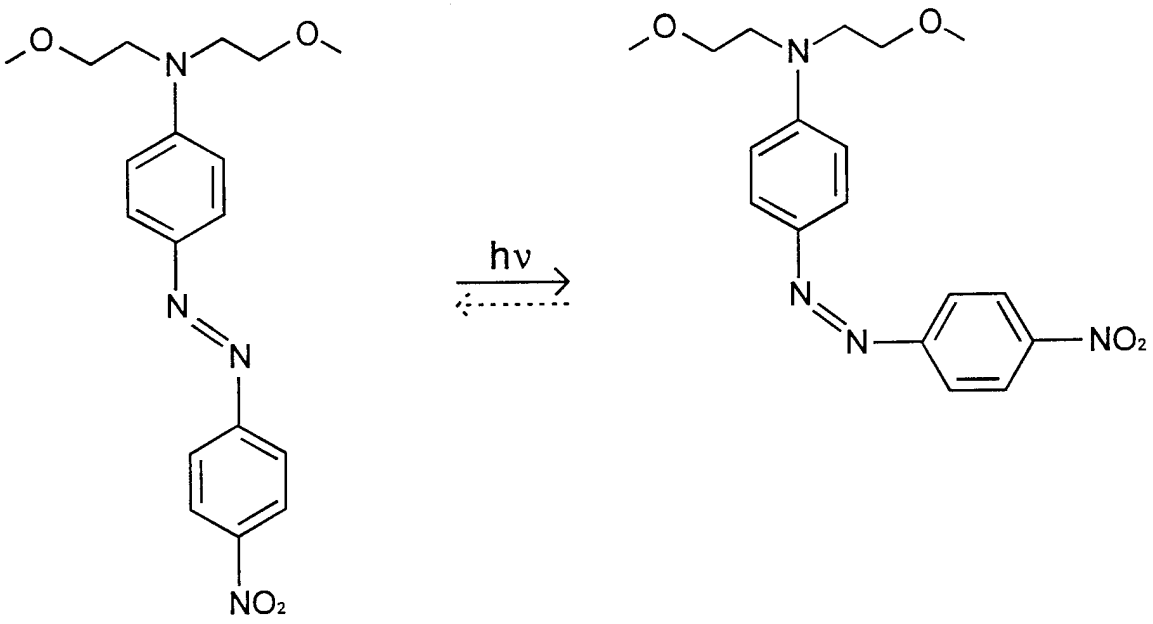

Figure 3. Photoisomerization of the DR19 chromophore.

The photoisomerization of the DR19 chromophore can be partially reversed by thermal annealing along with some recovery of the second order NLO activity (Chen et al, 1991). For this reason, temperature-insensitive photoprocessing with PUDR19 will require deliberate excess photoprocessing so that the desired Δn gradients will remain following thermal annealing. The PUDR19 polymer is a good choice for demonstrating this new processing approach since this polymer is well characterized and available in high purity. Success with this processing approach will attract attention to the need for a high $\mu\beta$ chromophore which undergoes irreversible photoprocessing. Thus, the temperature stability of photoprocessing is an issue which will need to be addressed with future polymers, but may be unnecessary to address specifically for the PUDR19 polymers as these polymers may be abandoned in favor of newer polymers containing high $\mu\beta$ chromophores. An alternative view is that improvements in the photoprocessing stability of existing polymers may allow the realization of low drive voltage, low insertion loss EO polymer devices with current NLO polymer technology. Since the potential importance of photoprocessing stability has not been previously articulated, little research has gone in this direction. The high desirability of low cost, high efficiency and high quality single step optical-only fabrications involving complex waveguide structures will result in NLO polymers developed specifically for this purpose which will have the desired secondary characteristics including

temperature stability. These materials may indeed follow some of the footsteps of industrial photoresist technology development.

3.2 POSITIVE PHOTORESISTS AS A PROCESSING MODEL

Photochemical processing can be used to fabricate a buried channel waveguides and other structures directly without deposition of a cladding layer. This procedure involves multicolor processing with the use of a mask in one step. The development of a buried channel in an NLO polymer by photoprocessing depends upon the fact that the penetration of the radiation into the sample will depend upon radiation wavelength. Explicitly, the time-dependent spatial concentrations of bleached and unbleached NLO chromophores in films can be modeled to good approximation by the following coupled equations (Dill et al., 1975):

$$\partial I(x,t)/\partial x = -I(x,t)\left[a_{cis}C_{cis}(x,t) + a_{trans}C_{trans}(x,t) + a_{poly}C_{poly}(x,t)\right]$$

$$-\partial C_{cis}(x,t)/\partial t = \partial C_{trans}(x,t)/\partial t = -\alpha C_{trans}(x,t)\, I(x,t)$$

where I(x,t) is the depth- and time-dependent light intensity, the a's are molar absorptions for the cis and trans forms of the NLO chromophore and other absorption by the polymer, the C's are depth- and time-dependent concentrations, and α is the photoconversion rate per unit intensity. For example, these equations provide a very good description of the photochemical properties of the USC polymers containing DR19 (Chen et al., 1991).

Representative data for light transmission as a function of depth into the NLO polymer film are shown in Figure 4 for a DR19-containing polymer (Chen et al., 1991, polymer #3). β is the effective absorption coefficient; β in this figure is defined as the optical density at a given wavelength normalized to the optical density at the absorption maximum near 475 nm. By reducing β, light is less attenuated and the resulting photochemical reactions have gradients which follow the more penetrating profile of the light in the film. As an example, the PUDR19 films typically have a transmission of 10% at 475 nm through a film thickness of approximately 800 nm. This results in a steep gradient of light intensity within the film as illustrated by the $\beta = 1$ curve in Figure 4.

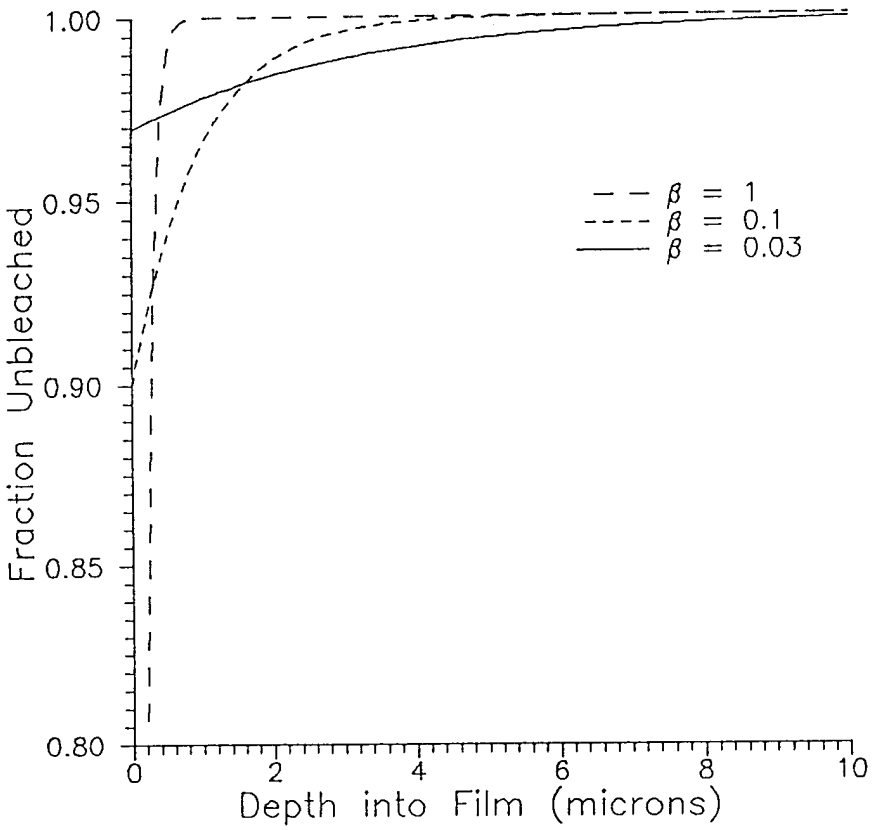

Figure 4. Photoprocessing of an NLO polymer film as a function of wavelength.

An illustration of a multicolor lithography process is shown in Figure 5. The first step involves the use of a strongly absorbing wavelength to photoprocess the top surface of the NLO film to create a cladding layer of lower index. The attenuation of the light into the depth of the film results in a smooth, graded index transition from the low index processed region to the higher index of the bulk of the film. The resulting graded index profile is illustrated in the bottom left of Figure 5. This first exposure can be spatially confined as suggested in the illustration, or it can extend uniformly over the entire surface to photoprocess a uniform cladding layer within the NLO film over the extent of the film. This latter example can be accomplished by the "flood" exposure provided over an entire substrate by a UV exposure system used for processing photoresists, a standard piece of equipment in the semiconductor industry. With either large or small exposure areas, the total exposure can be varied to change the depth of the Δn gradient.

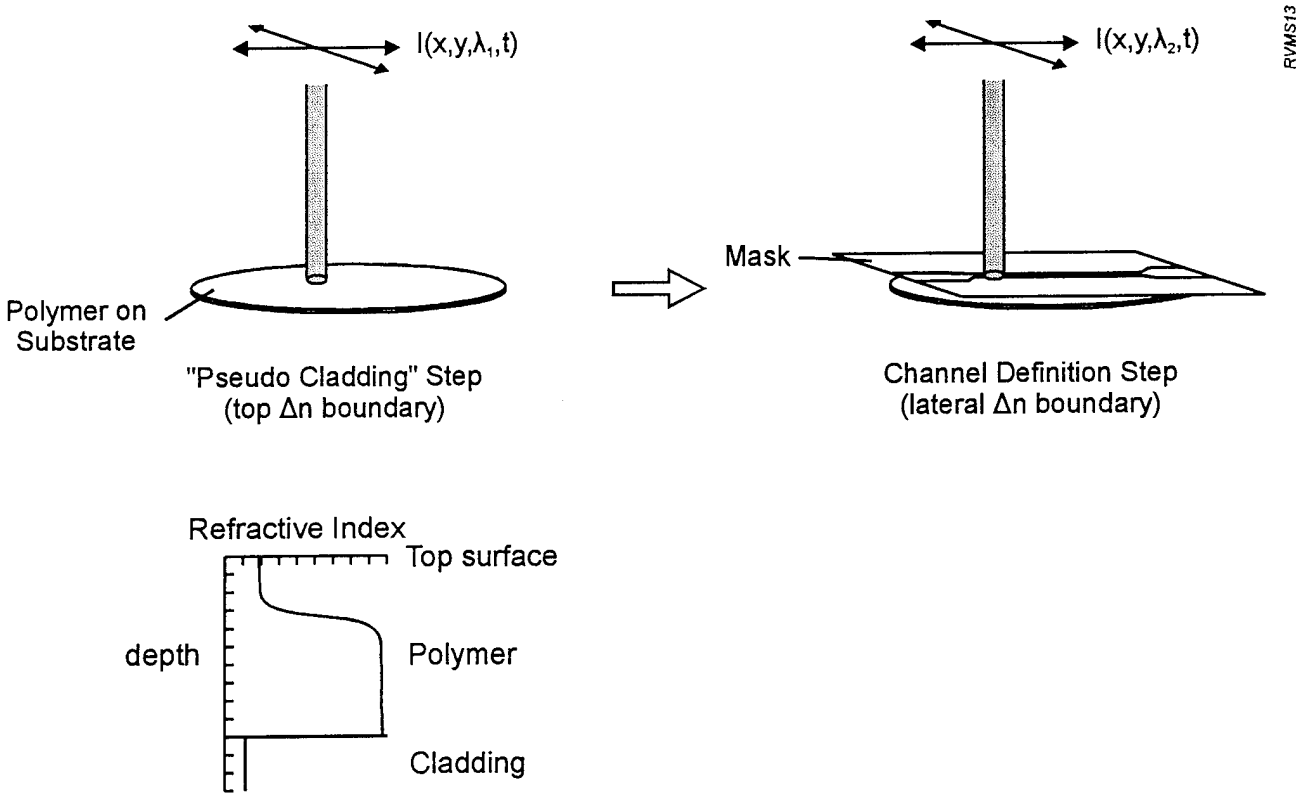

Figure 5. Illustration of multicolor lithographic processing of waveguide structures in NLO polymer films.

Moving from the bottom to the top of the material (Figure 5, bottom left), one finds (1) the lower cladding layer, (2) the unbleached, high index, EO active channel, and (3) the bleached, low-index upper layer. This approach leaves a high index region which forms a buried waveguide in the NLO film. Note that the waveguiding region has not been bleached. This leaves the NLO activity of the waveguiding region of the polymer unaffected by the photoprocessing.

In the second step shown in Figure 5, a light field mask is used to photoprocess the regions of the NLO film surrounding the waveguide with a penetrating, highly transmissive wavelength. This exposure results in a small Δn gradient as illustrated in Figure 4 ($\beta = 0.03$, for example) which provides the lateral definition of channel waveguides in the NLO film by replicating the pattern of the light field mask. Additional exposures without the mask can be used to further shape the Δn profiles between clear field and dark field mask features.

The process in Figure 5 has many important features which contrast it with current methods of channel waveguide fabrication. First, it is an all optical process involving a minimum number of steps. This can have a large impact on fabrication cost and optical quality of the waveguides. The photoprocessing steps for fabricating waveguides in NLO polymers are contrasted with the steps for conventional fabrication using dielectric etching in Table 1. The optical only processing involves few steps and low cost equipment. By contrast, while photoresist processing in the etching approach requires similar cost equipment, the plasma etching adds additional cost, and the added process steps further add to the fabrication cost and complexity.

Optical quality of the waveguide is very sensitive to the processing. In the case of etching, the wall roughness must be carefully controlled to minimize optical losses. While ion cyclotron etching has improved wall smoothness, the optical only process results in inherently smooth waveguide boundaries owing to the diffractive properties of light at the edges of mask features. Figure 6 shows the intensity gradient beneath a typical mask feature resulting from diffraction of the light at the mask boundary (Born & Wolf, 1980). Directly beneath the shadow

NLO WAVEGUIDE PROCESSING STEPS	
MULTICOLOR LITHOGRAPHY	CONVENTIONAL PROCESSING
spin coat bottom cladding	spin coat bottom cladding
spin coat NLO polymer	spin coat photoresist
first exposure (λ_1)	soft bake
second exposure (λ_2, mask)	expose photoresist (UV, mask)
	wet process photoresist
	plasma etch
	strip photoresist
	spin coat NLO polymer
	spin coat top cladding layer

Table 1. Comparison of processing steps with conventional waveguide processing.

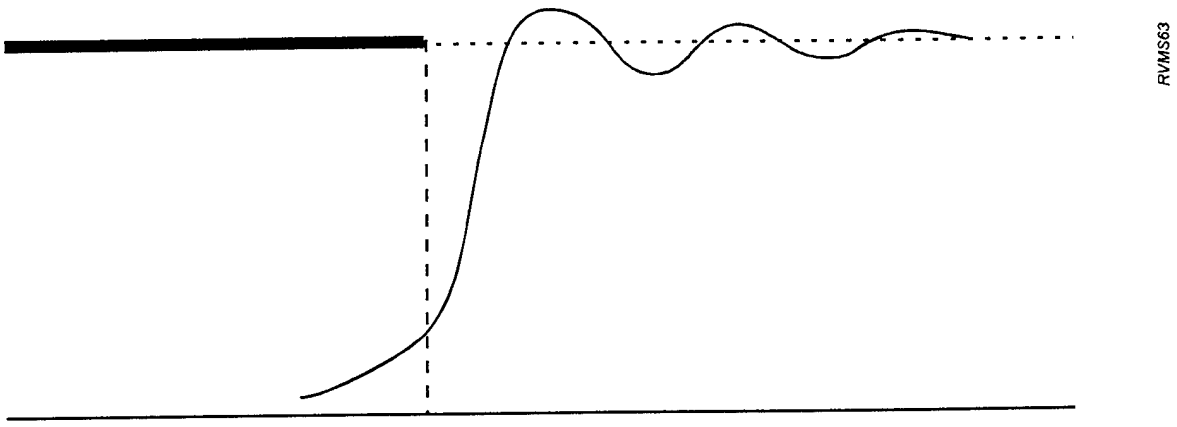

Figure 6. Intensity gradients in the shadow edges of lithographic mask features.

edge of the mask feature, the electric field of the incident light falls to 50%. The edge of the mask feature basically propagates a cylindrical electromagnetic wave which interferes with the incident plane wave to result in the decaying standing wave, the field gradient beneath the edge, and the decaying field underneath the mask feature. The squaring of the field to calculate the exposure intensity results in a gradient which falls to 25% directly beneath the mask edge. The gradient depends upon wavelength and distance. The example shown in Figure 6 is for a distance of 6 wavelengths below the mask.

Since the best known examples of low loss waveguides are based on the use of graded index rather than step index waveguides, we expect the optical propagation losses in optically photoprocessed waveguides to provide competitive (if not the very lowest) waveguide losses in NLO polymers. This expectation is based on the successes of low loss fibers and in-diffused waveguide structures in crystalline inorganics such as lithium niobate. Both of these examples have graded index waveguides in which the Δn boundaries of the waveguides are smooth gradients created by the diffusion of dopants. Refractive index gradients formed by multicolor lithography of NLO polymers have similar microscopic homogeneity and should be capable of providing minimal excess losses due light scattering in waveguides.

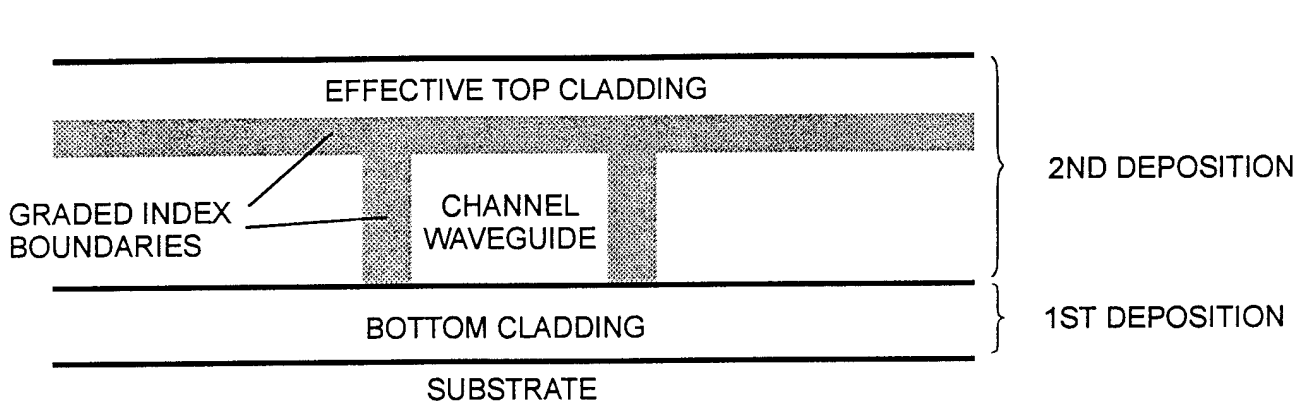

Figure 7. Graded index waveguide boundaries resulting from photoprocessing.

Figure 7 shows a cross section of a waveguide fabricated by the multicolor lithography described in Figure 5. The horizontal gray zone is the graded index resulting from the first exposure using a strongly absorbing wavelength. This creates the effective top cladding. The second exposure with the high transmission wavelength results in the vertical index gradients of small Δn which laterally define the channel waveguide. The only mechanically defined waveguide boundary is the bottom boundary of the waveguide created by the first deposition. Since this deposition is the first step of the polymer film process, this film can normally achieve extremely low roughness. It should be pointed out, however, that for some cases such as waveguide structures on a transparent substrate such as glass or glass/indium tin oxide, the photoprocessing can also be applied from the underside to provide graded index boundaries on all sides of the waveguide. This may particularly offer advantages in processing low loss passive waveguides.

Besides simplified, lower cost processing and optical loss benefits, the multicolor lithography process importantly provides the capability to spatially vary the Δn gradients within a single film to "sculpt" waveguides of different sizes while keeping them single mode through control of the magnitude of Δn. This will have a direct impact on the ability to optically fabricate advanced waveguide structures such as low loss taper transitions between large single mode waveguides for fiber and small waveguides between closely spaced electrodes for maximizing the EO response as shown earlier in Figure 2. Further, the ability to tailor cladding layers

from the NLO polymer can alleviate fabrication difficulties where custom claddings are needed in order to provide mode control as well as electrical conduction which matches that of the NLO core layer for avoiding cladding interference with poling.

3.3 MULTICOLOR PROCESSING AND REFRACTIVE INDEX GRADIENT CONTROL

To validate the multicolor lithography process for refractive index control, it is necessary to demonstrate that the photoprocessing can be performed over a meaningfully wide excursion of wavelength (i.e., β in Figure 4). All previous photoprocessing research with NLO polymers was done with UV photomask aligners using standard, high pressure mercury arc lamps for light sources (Chen et al, 1991). Typical photoresist exposure systems used in this early work provide 10's of mW/cm^2 output in a uniform field over the surface of a wafer. The band at 405 nm comprises approximately 2/3 of the spectral output intensity, and the remaining third comes from the band at 365 nm (Chen et al, 1991). While 405 nm is in the "valley" of the UV-visible absorption spectrum between the strong UV absorption and the visible absorption, the significant presence of the strongly absorbed 365 nm light precludes a simple and direct analysis of the wavelength dependence of the published photoresist kinetics using this mixed wavelength exposure.

The kinetics described in Section 3.2 were therefore analyzed over an excursion of discrete wavelengths using a variety of lasers as exposure sources. An attempt was made using an inexpensive high pressure sodium lamp to expose the NLO polymer at 580 nm using a narrow pass filter, but the output power was too weak following the collection optics and narrow band pass filter. The kinetics with this weak source (~1 mW/cm^2) were too close to the noise level of the spectrophotometers for reliable measurements over time spans of 10's of minutes to hours. Lasers with powers in the range of 20 mW/cm^2 provided significant photoprocessing results which could be easily measured with spectrophotometers.

All PUDR19 samples were synthesized by Prof. Larry Dalton and his co-workers at USC. Thin films of 0.7 μm thickness were prepared on 1 inch glass slides or glass/indium tin oxide slides. Photoprocessing kinetics were measured on both poled and unpoled films. Photoprocessing was effective on both poled and unpoled films. This finding is consistent with previous measurements with UV photoprocessing of these materials by USC.

Using argon ion lasers at the wavelengths of 488 nm and 515 nm, the photoprocessing kinetics were measured by using a pump-probe experimental arrangement in which the transmission at low intensity of one wavelength is measured during an exposure using a high intensity of the other wavelength. The results for such an experiment exposing the film at 488 nm while measuring the transmission at 515 nm is shown in Figure 8. The exposure intensity of 20 mW/cm^2 results in a rapid photobleaching of the polymer. The initial slope is steep and the final value of the transmission is 76%, a value indicating a large conversion of the trans chromophore to the cis isomer. The difference between initial and final values suggests a photoconversion of ~90% of the chromophore from trans to cis.

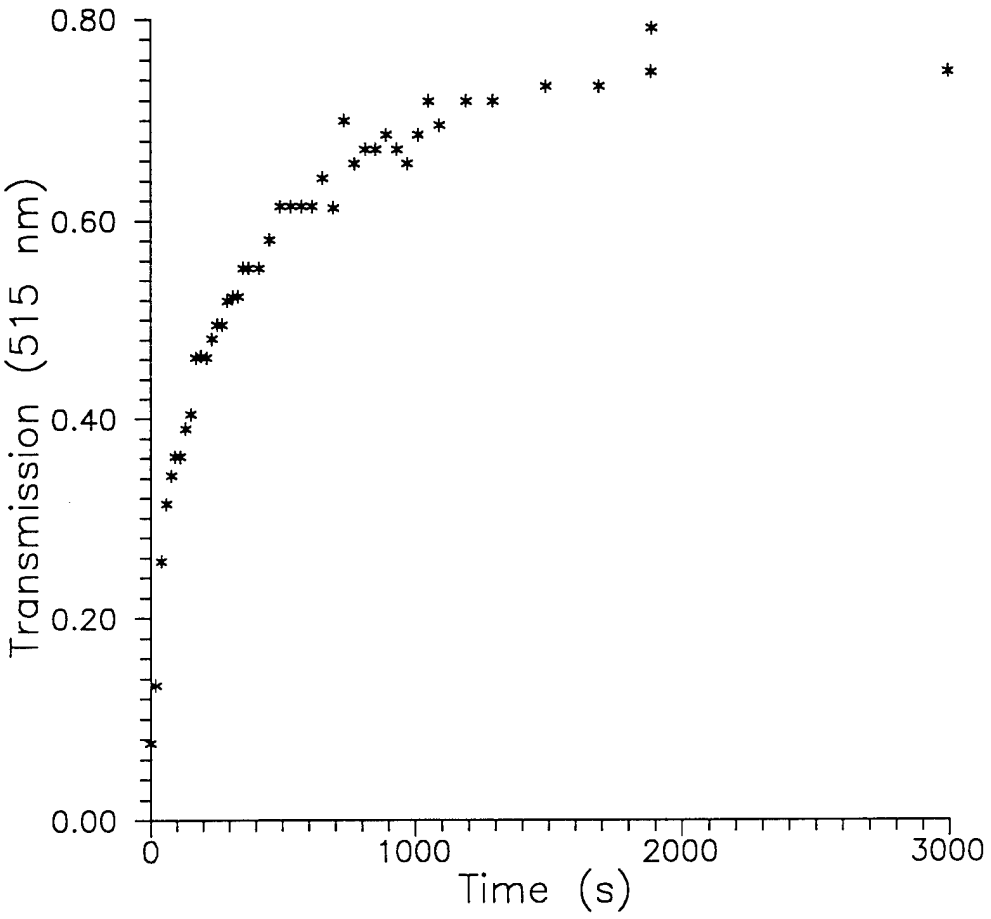

Figure 8. Photoprocessing kinetics of PUDR19 at 488 nm.

This photoconversion of trans to cis is significantly greater than the conversion indicated in published data using mixed wavelength UV illumination. In this published data (Chen et al., 1991), the limiting photoconversion was limited to ~50%, a value suggesting that the photoisomerization of cis to trans was also occurring. While the 405 nm component is in the short wavelength side of the trans absorption maximum at 475 nm, the 365 nm exposure component is clearly in the edge of the strong UV absorption bands below 400 nm. The selective excitation of the trans isomer may account for the higher photoconversion of trans to cis at longer wavelengths such as 488 nm.

The kinetics measured for a similar pump-probe experiment with the intensities reversed is shown in Figure 9. In this experiment the exposure was made with 515 nm laser light while monitoring the transmission at 488 nm. Again, the photoprocessing kinetics are rapid. The 515 nm exposure was also made using a power of 20 mW/cm^2.

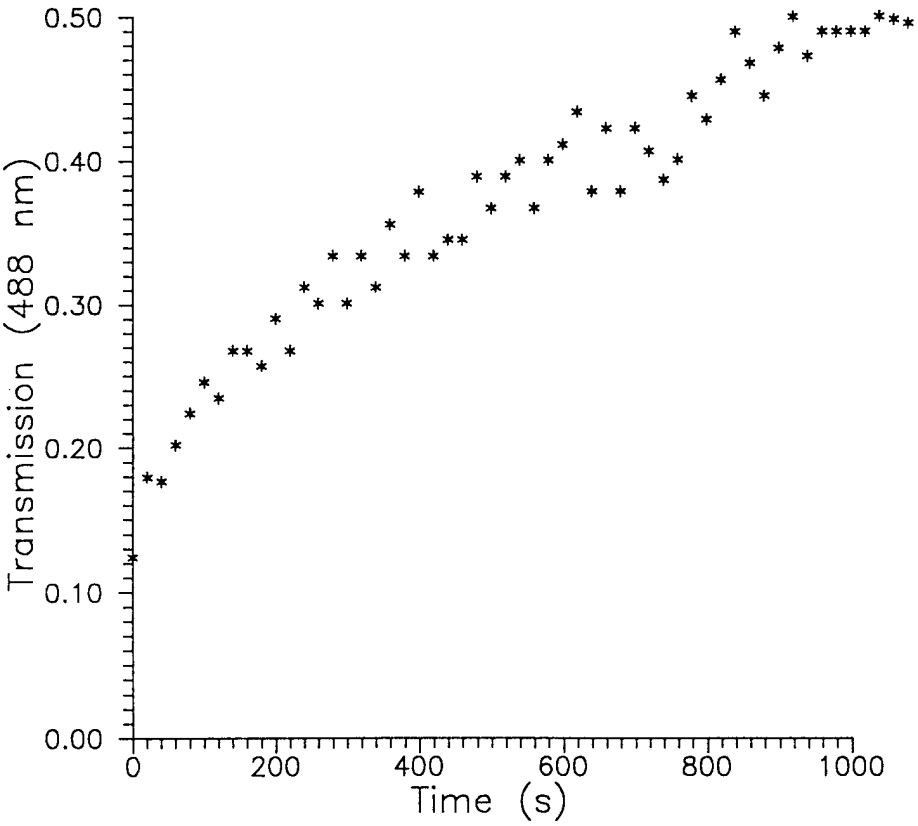

Figure 9. Photoprocessing kinetics of PUDR19 at 515 nm.

Both 488 nm and 515 nm are relatively close to the trans absorption maximum at 475 nm. For this reason, the refractive index gradients resulting from photoprocessing at these wavelengths are relatively large and are not greatly different. To demonstrate photoprocessing of small Δn gradients using highly penetrating light, photoprocessing experiments were conducted with a frequency doubled YAG laser. In the short pulse mode, the intensities were too great and film damage was observed. Turning off the Q switching, lower intensity exposures of the PUDR19 films could be made in the long pulse mode. The photoprocessing was monitored by repeated measurements of the transmission of the samples using a spectrophotometer following exposures.

The response of the PUDR19 films to exposure at 532 nm is shown in Figure 10. The region of the absorption maximum is plotted for exposures up to 70 minutes. The absorbance falls monotonically with exposure as expected.

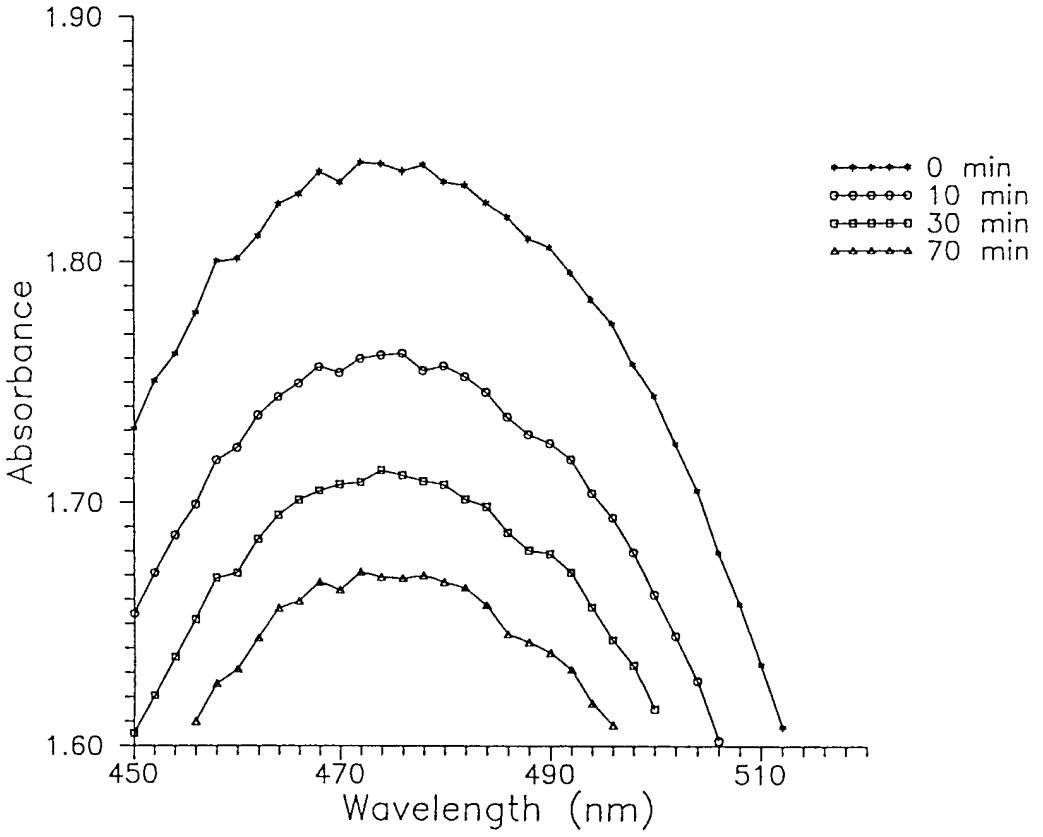

Figure 10. Photoprocessing kinetics of PUDR19 at 532 nm.

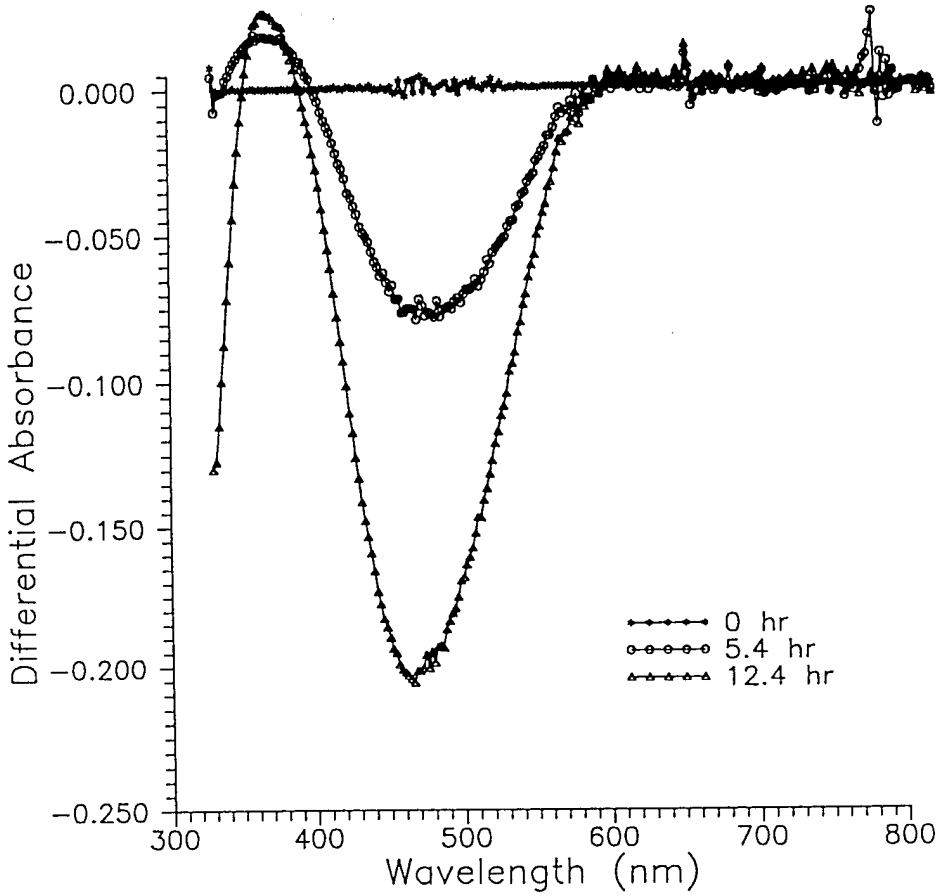

Figure 11. Later time photoprocessing kinetics of PUDR19 at 532 nm.

To demonstrate that this process continues beyond the initial 70 minutes shown in Figure 10, long time exposures were made in another experiment using 532 nm light. In this experiment, the "doughnut" mode intensity profile was made uniform by passing the laser light through a fiber optic and refocusing the fiber output on the sample. This lowered the exposure intensity to 1.5 mW/cm^2. The results were recorded using the differential absorbance mode of the spectrophotometer and are shown in Figure 11. The falling absorption corresponds to the loss of the trans isomer at 475 nm. The photoprocessing clearly is continuing on the time scale of hours using this exposure.

To further demonstrate photoprocessing at an even longer wavelength, a 20 mW/cm^2 exposure of a PUDR19 sample using a dye laser was performed. Absorption measurements were made of the sample following a series of 570 nm

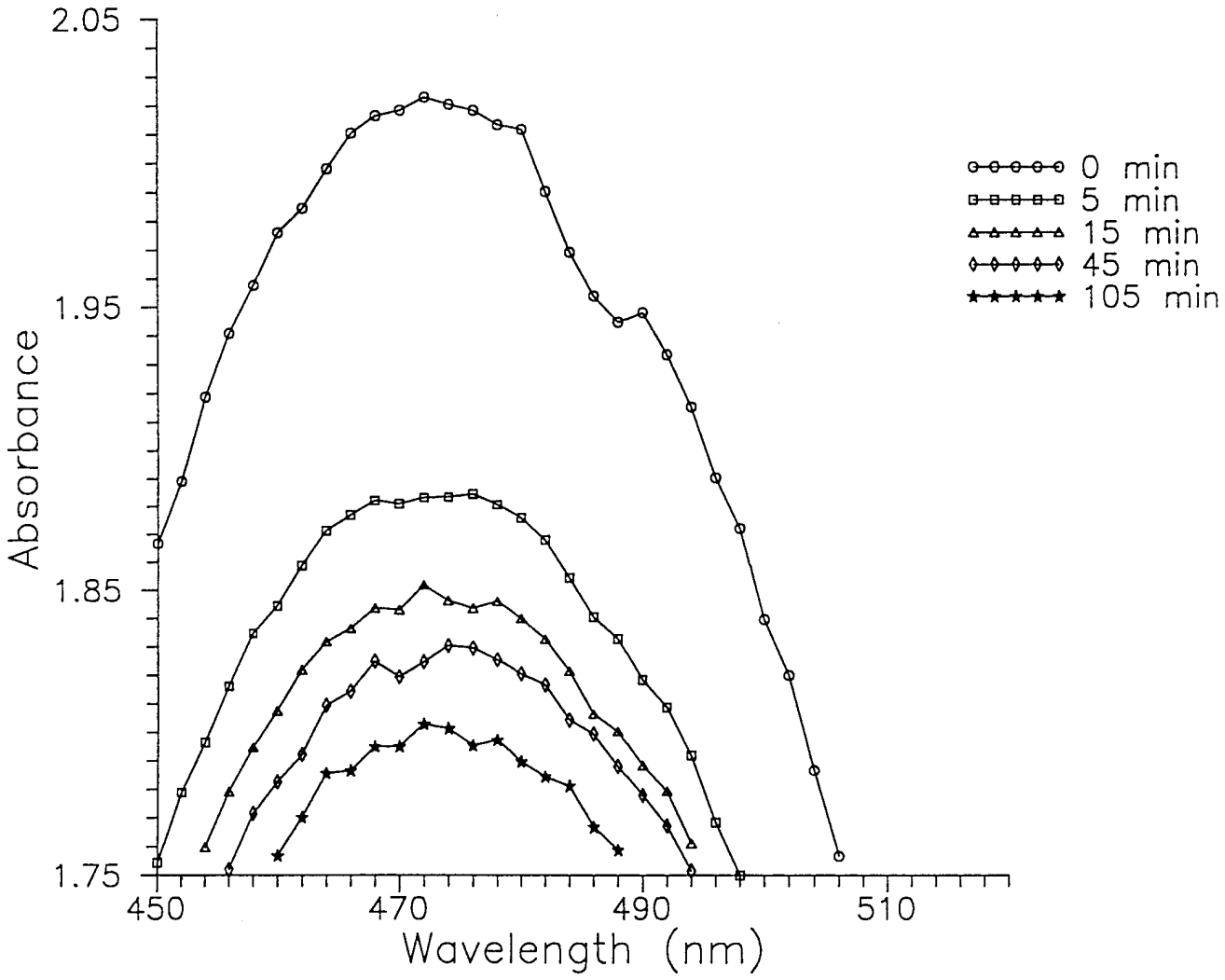

Figure 12. Photoprocessing kinetics of PUDR19 at 570 nm.

exposures. The absorption spectra are shown in Figure 12. Again, the exposure results in a monotonic decrease in the trans isomer absorption. Following the initial short exposure, a slow rate of change was observed as a function of exposure time. The small and rapid initial change is unexplained, but may be related to a small heterogeneity of the PUDR19 chromophore in the polymer which undergoes a more rapid photobleaching.

The kinetics can be analyzed with respect to the photoresist response model by rearranging the kinetics equations to the following forms (Dill et al., 1975):

$$A = (1/d)\ln[T(\infty)/T(0)]$$

$$B = -(1/d)\ln T(\infty)$$

$$C = \frac{A+B}{AI_0T(0)[1-T(0)]}\frac{dT(0)}{dt}$$

where

$$A = (a_{trans}-a_{cis})C_{trans}(0)$$

$$B = a_{poly}C_{poly}(0)+a_{cis}C_{cis}(0)$$

and C, the fractional decay rate, is defined as earlier. A and B have the units of μm^{-1} and C has units of cm^2/mJ. Because the argon ion pump-probe experiments were not measuring the transmission at 475 nm, the results of these experiments were corrected to 475 nm absorption and transmission values using the absorption spectrum for the trans chromophore.

The resulting plots for the early time transmission kinetics used in the calculation of C, the trans-to-cis isomerization rate, are shown in Figures 13-16 for wavelengths 488 nm, 515 nm, 532 nm and 570 nm, respectively. The slopes fall rapidly with increasing wavelength as the photoprocessing becomes less efficient at higher wavelengths. The calculated results for the kinetics model parameters are shown in Table 2. While the values of A and B follow the absorption spectra, the photoprocessing rate, C, falls very rapidly with increasing wavelength. For reference, these different wavelengths relative to the PUDR19 absorption spectrum are shown in Figure 17. These results span a sufficiently wide range of

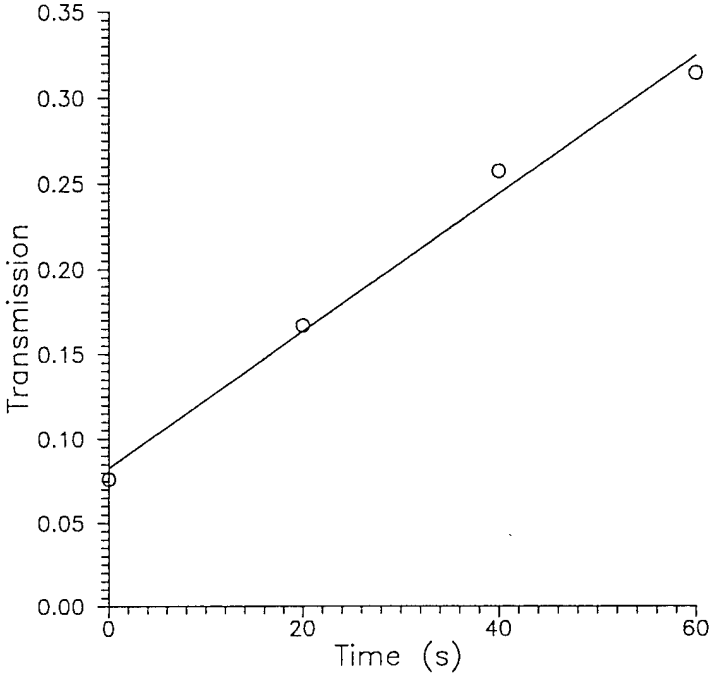

Figure 13. Early time photoprocessing kinetics at 488 nm.

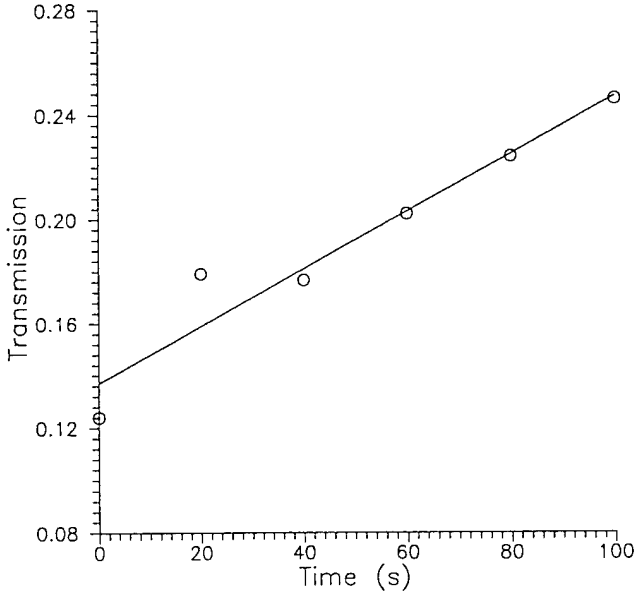

Figure 14. Early time photoprocessing kinetics at 515 nm.

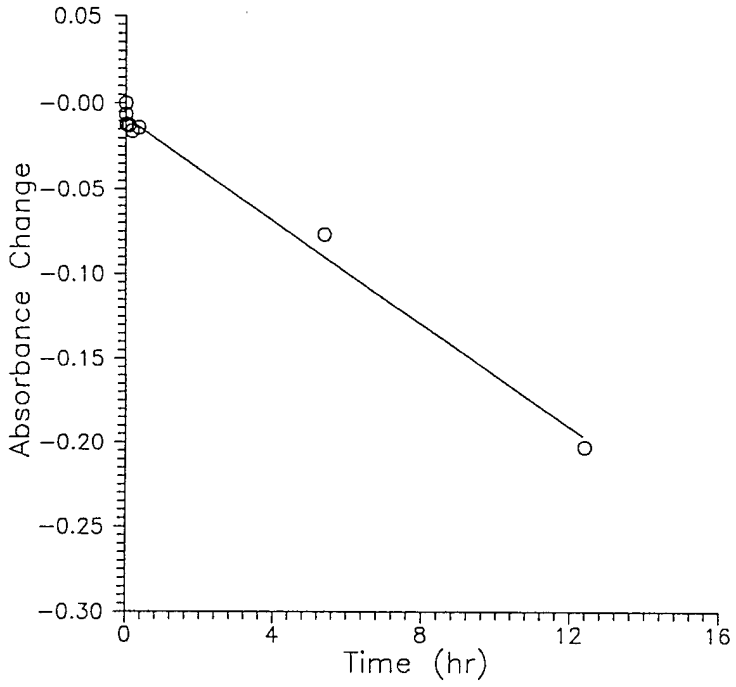

Figure 15. Early time photoprocessing kinetics at 532 nm.

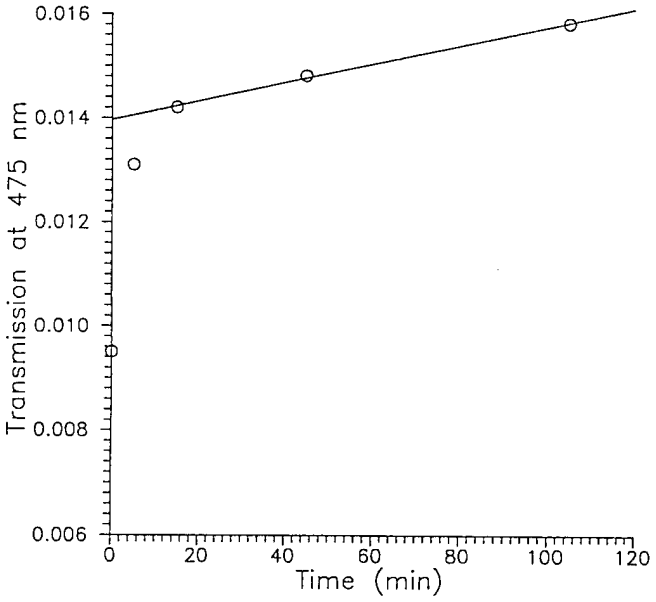

Figure 16. Early time photoprocessing kinetics at 570 nm.

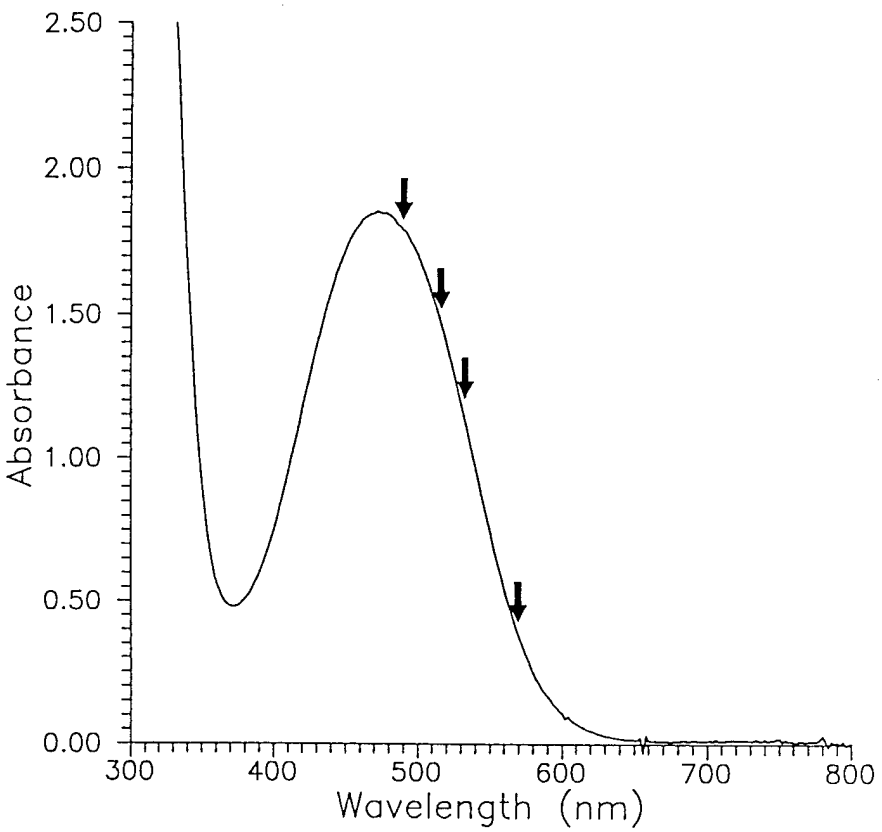

Figure 17. Wavelengths used for kinetics measurements relative to the PUDR19 absorption spectrum.

wavelength to demonstrate photoprocessing into the red edge of the absorption band at relatively penetrating wavelengths.

A plot of the photoprocessing rates, C, vs. wavelength from Table 2 is shown in Figure 18. While the decrease in rates is very rapid at longer wavelengths, the rates are still sufficiently rapid to allow sizable refractive index gradient fabrications in PUDR19 films through the use of laser illumination. Standard commercial dye lasers typically deliver 0.5 W or more of power using a 5-6 W argon ion laser as a pumping source. Such systems have approximately the same cost as a UV mask aligner. By focusing the beams down to beam sizes of approximately 0.1-1 mm, photoprocessing of NLO polymer films is calculated to require on the order of minutes to 10's of minutes at deeply penetrating wavelengths approaching 600 nm. This is well matched to typical rhodamine 6G dye laser outputs which reach maximum output at wavelengths > 585 nm.

PHOTOPROCESSING KINETICS PARAMETERS			
Wavelength	A (μm^{-1})	B (μm^{-1})	C (cm^2/mJ)
488	2.94	2.94	6.4×10^{-3}
515	2.54	2.54	1.8×10^{-3}
532	2.02	2.02	4.0×10^{-4}
570	0.65	0.65	2.9×10^{-6}
405 + 365	5.5	5.5	6.7×10^{-3}

Table 2. Photoprocessing kinetics parameters based on Dill's analysis of positive photoresists.

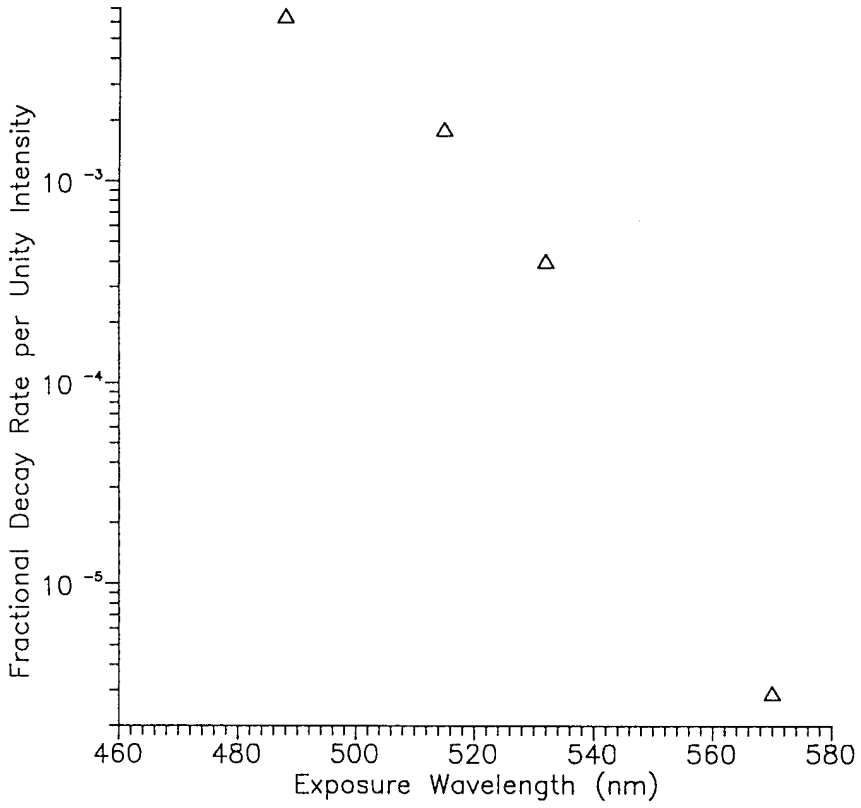

Figure 18. Demonstration of photoprocessing at high penetration wavelengths.

Two important implications of the slow photoprocessing rates at deeply penetrating wavelengths are the inherent control of the processing and waveguide insensitivity to near infrared light. Good process control for the precision exposure of waveguide features and 3-D structures is inherent because of the relatively low sensitivity of the photoprocessing at these wavelengths. Fabrication processes are more precisely controlled when the timing requirements are in seconds or minutes rather than microseconds to milliseconds. This provides integrated exposure control and also allows multiple exposures at different wavelengths and spatial positions to be used to "smooth" the resulting refractive index gradients within the films. Secondly, this relative insensitivity suggests that low level exposure of films to ambient light and much higher levels of waveguided infrared light will not adversely impact the films. This has recently been demonstrated in the research by TACAN Corporation where they have demonstrated stable operation of prototype DR19-containing NLO polymer modulators at power levels of 10 mW of 1.3 μm light in a channel waveguide for extended periods of time (Shi, 1996). Together, these results indicate that photoprocessing will provide good process control along with the inherent advantages of all optical processing which includes low fabrication cost, high film quality, ease of advanced waveguide structure fabrication, and graded index waveguides having low optical losses.

3.4 MICROSTRUCTURE APPLICATION RESULTS

The 3-D capabilities of the photoprocessing of NLO polymers offers unique advantages over other processing approaches for the fabrication of more complex waveguide structures. In particular, the vertical taper (described earlier in Figure 2) which can transition a large single mode down to a small single mode offers a unique solution to an Air Force-stated need for small NLO polymer waveguides between closely spaced electrodes (Caracci, 1996; Grote, 1996). Such tightly confined waveguides will greatly reduce drive voltages for NLO polymers down to the levels needed for devices. Conventional etching techniques can be used to fabricate advanced structures, but these methods are generally limited to 2-D patterning. The unique ability to spatially confine a light beam and vary its exposure over a surface gives photoprocessing the unique ability to vary waveguide structures in all three dimensions in a NLO polymer film.

A demonstration of the photoprocessing required for fabricating a vertical taper was conducted by translating a laser beam across a sample with varying exposure times. The frequency double output from a YAG laser in the long pulse mode was focused with a long focal length lens to a 2.5 mm spot. A 2.0 mm

aperture was placed at the focal position and the NLO polymer films was placed behind the aperture on a translation stage. The sample was then translated in 400 μm steps behind the aperture. The step size is shown to scale in the illustration. The exposure time at each step was varied to create an exposure gradient. Then by spatially measuring the photoconversion of the NLO chromophore, the presence of a vertical taper resulting from an exposure gradient was verified.

Figure 19 shows the result for a vertical taper resulting from a sequence of linearly increasing exposures over a distance of 4 mm. The absorption of the film at 475 nm decreases over this distance. Converting this absorption decrease to a change in the integrated refractive index profile of the film results in a change of -0.04 for a maximum exposure. This maximum change corresponds to an approximately 42% photoconversion at the surface of the film, equivalent to Δn of 0.10. The refractive index profile is shown in Figure 20 for different distances along the taper.

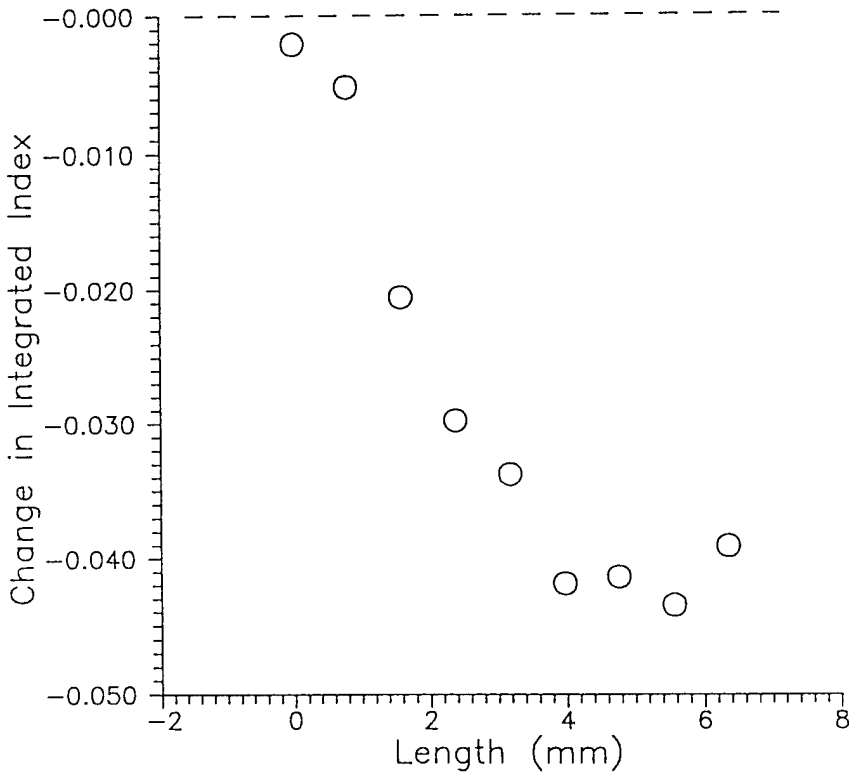

Figure 19. Large photoprocessed refractive index taper within a PUDR19 polymer film.

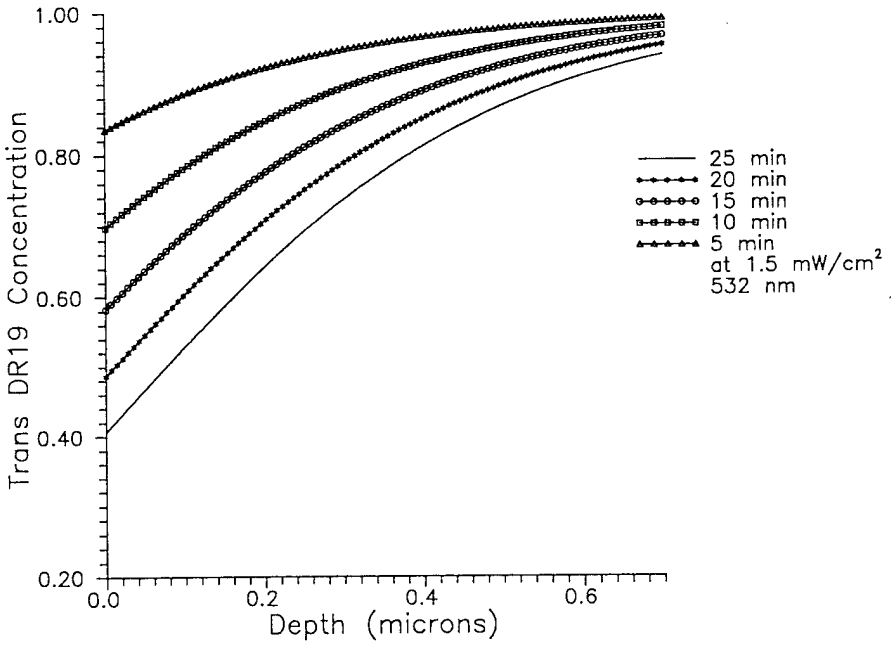

Figure 20. Example refractive index profiles within the exposure taper.

Demonstration of a small magnitude vertical taper in the index is shown in Figures 21 and 22. Figure 21 shows a surface plot of a gradual exposure gradient spanning approximately 8 mm as the sample is translated behind the 2.0 mm aperture. Absorption measurements of the peak absorbance (475 nm) were scanned before and after exposure and are shown in Figure 22. Because the measurement error in the differential absorption measures are large compared to the exposure gradient, the exposure gradient is included in the figure to illustrate the profile of the taper. As expected, gradients of any magnitude within the photoprocessible range of Δn are easily processed using this approach.

These experiments demonstrate that the exposure gradients required for fabricating vertical taper transitions to buried waveguides can be easily made by varying the spatial exposure of the NLO film. This is a capability unique to photoprocessing which permits the variation of refractive index gradients in the third (i.e., depth) dimension throughout the NLO film. Besides the direct fabrication of waveguide tapers, this process can be applied to complex waveguide structures such as branches, buried waveguides, and gratings. Some specific applications are discussed further in the conclusions/recommendations section of this report.

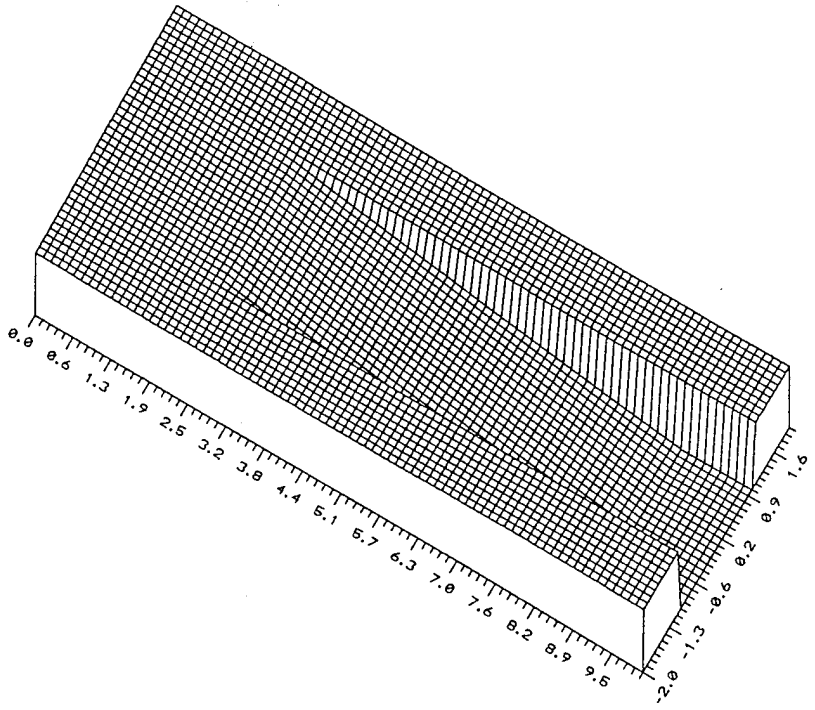

Figure 21. Surface plot of exposure profile for a small magnitude vertical taper.

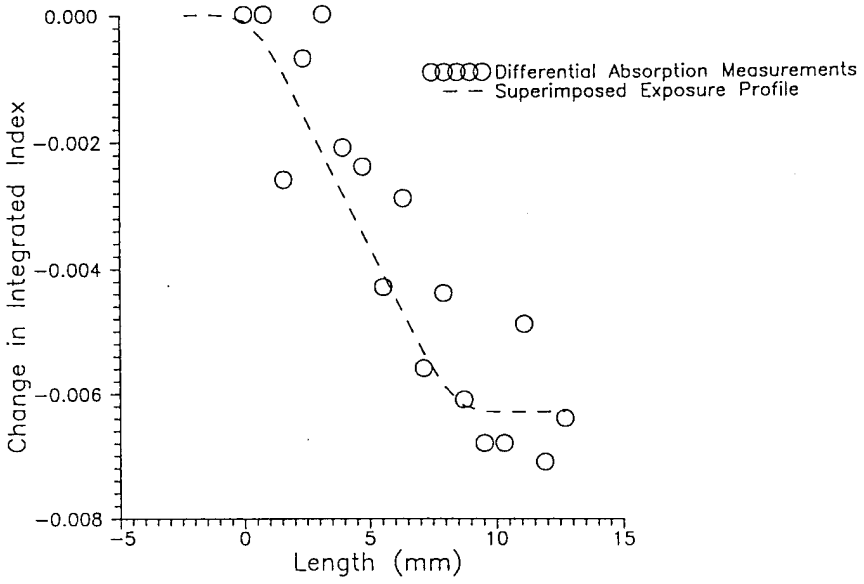

Figure 22. Measured refractive index profile for the exposure profile shown in Figure 21.

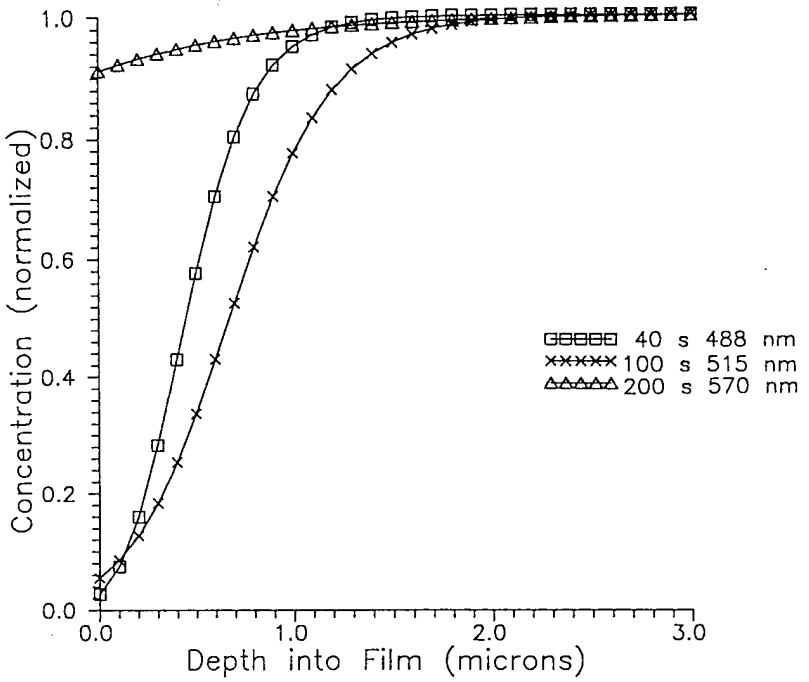

Figure 23. Refractive index profiles as a function of processing wavelength.

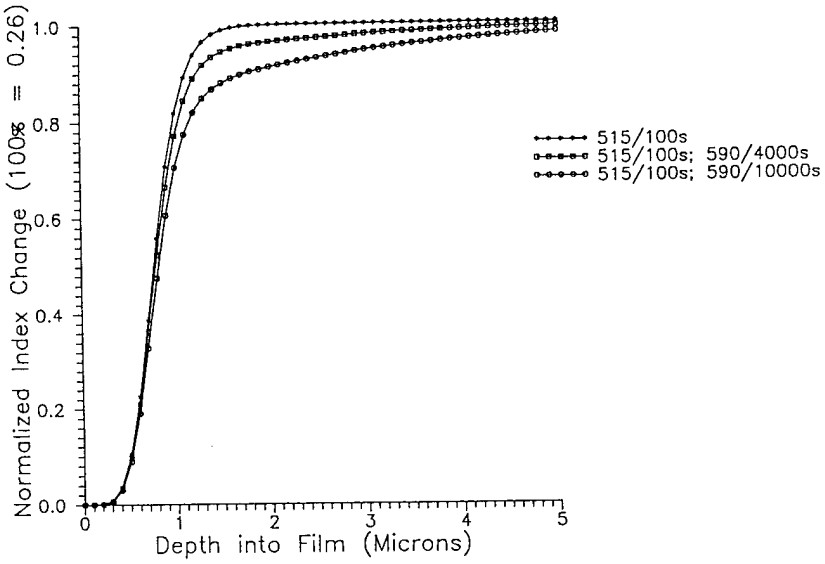

Figure 24. Refractive index profiles for multicolor photoprocessing at 515 nm and 590 nm.

In the second step, a light field mask is introduced and additional 590 nm exposure is made to result in the total exposure in Figure 24 corresponding to the longer 590 nm total exposure. The difference between the two 515+590 nm exposure curves in Figure 24 determine the lateral Δn gradient into the depth of the NLO film which define the buried channel waveguide. The shorter 590 nm exposure serves to "round" the profile and provide a more uniform front-to-back Δn gradient difference between the masked (channel) and unmasked exposure regions.

An example of the resulting refractive index profile in the film is shown in Figure 25. This surface plot shows the refractive index in a cross section of the film. The single mode waveguiding region is the high index region protected by the mask toward the back of the film. The sharp drop in index created by the shorter wavelength exposure creates an effective cladding layer at the top surface of the NLO film and buries the waveguide below the film surface. Buried waveguides typically have smaller Δn gradients, and in this case the optically defined gradients are qualitatively similar to the graded index gradients of low loss waveguides defined through diffusion processes in materials such as lithium niobate.

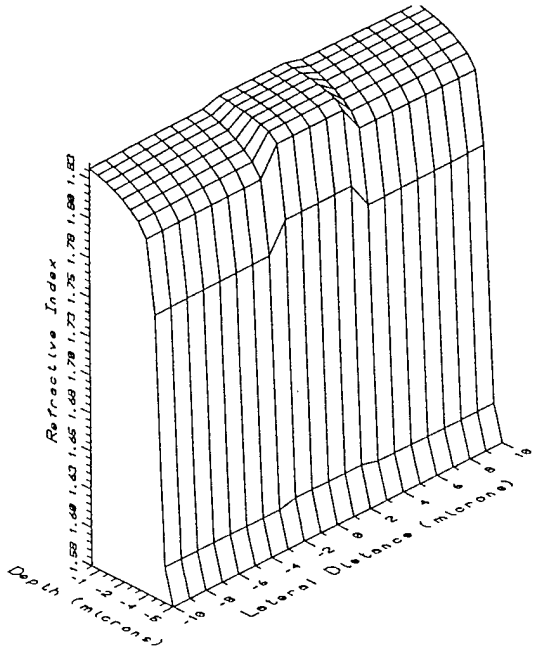

Figure 25. Refractive index in a cross section of a tapered channel waveguide.

The availability of >0.5 W of laser power at wavelengths > 585 nm using standard dye lasers indicates that this processing can be performed quickly and easily using dye lasers focused to spot sizes of 1 mm^2 or less, yet slowly enough that fine processing control can be applied to the fabrication. Since dye lasers are tunable, a range of wavelengths can easily be applied to the processing along with optical manipulations (angle of incidence, depth of focus, etc.) to further smooth the photoprocessed refractive index gradients to achieve very low loss waveguides. Either the pump wavelengths of the argon ion laser used for the dye laser or exposure from a standard mask aligner can be used for creating the large index gradients in the NLO film surfaces.

4.2 SIMPLE, LOW COST FABRICATION OF LOW LOSS WAVEGUIDE TRANSITIONS (TAPERS) BETWEEN EO DEVICES AND OPTICAL FIBERS

Section 3.4 of this report detailed the demonstration of a linear tapered exposure gradient into the depth of the film. By moving either the sample or the laser beam with computerized control of position and integrated exposure, tapers of any desired exposure profile can be created. Both movement approaches have been developed for laser milling and laser ablation applications.

Figure 26 illustrates the two-step all-optical process for fabricating a vertical taper in an NLO polymer. In the first step, an exposure gradient using a short wavelength creates a broad (relative to the channel width) vertical taper. The exposure for such a taper was demonstrated in Section 3.4 and shown graphically in Figure 22a. In the second step, a light field mask of the channel is lithographed with a long wavelength over the taper to create the small lateral Δn boundaries which define a buried channel in the taper. Importantly, an exposure gradient can also be applied to the long wavelength exposures so that the lateral refractive index gradients, illustrated in the figure as δn_i can be varied to maintain the desired mode support and relatively constant effective index of the guided mode in the channel. The smaller dimensions of the waveguide following the taper will require that $\delta n_2 > \delta n_1$ as illustrated in Figure 25. This is easily accommodated through control of the integrated exposure profile.

The principle fabrication objective of this vertical taper is a low optical loss transition to a waveguide within a small electrode spacing. Such a fabrication is illustrated in Figure 27. A large single mode waveguide in the NLO polymer is used to match the large mode sizes of single mode fiber as shown on the left. Coupling losses to single mode fiber are typically much less than 1 dB/end face.

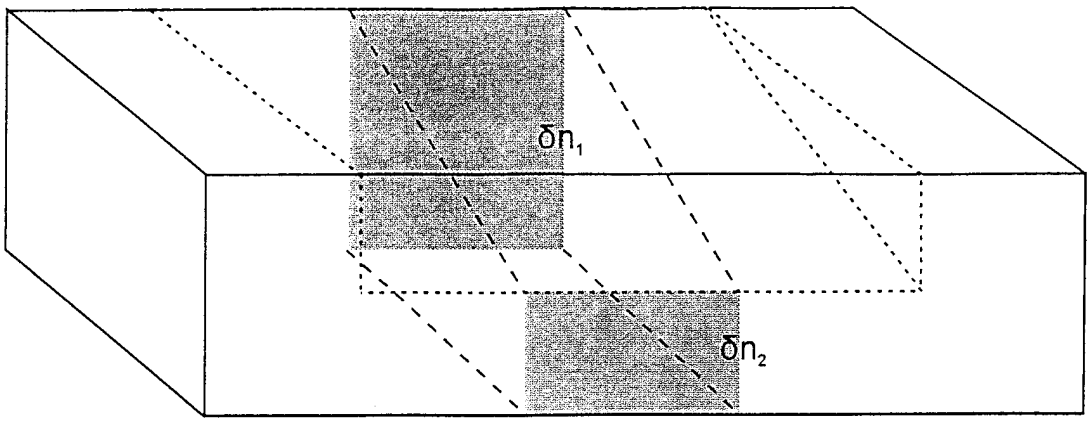

..... Step 1: Short wavelength exposure for descending upper index boundary

- - - - - - Step 2: Long wavelength exposure for vertical gradients to define channel

Figure 26. Two step process for a buried channel waveguide taper.

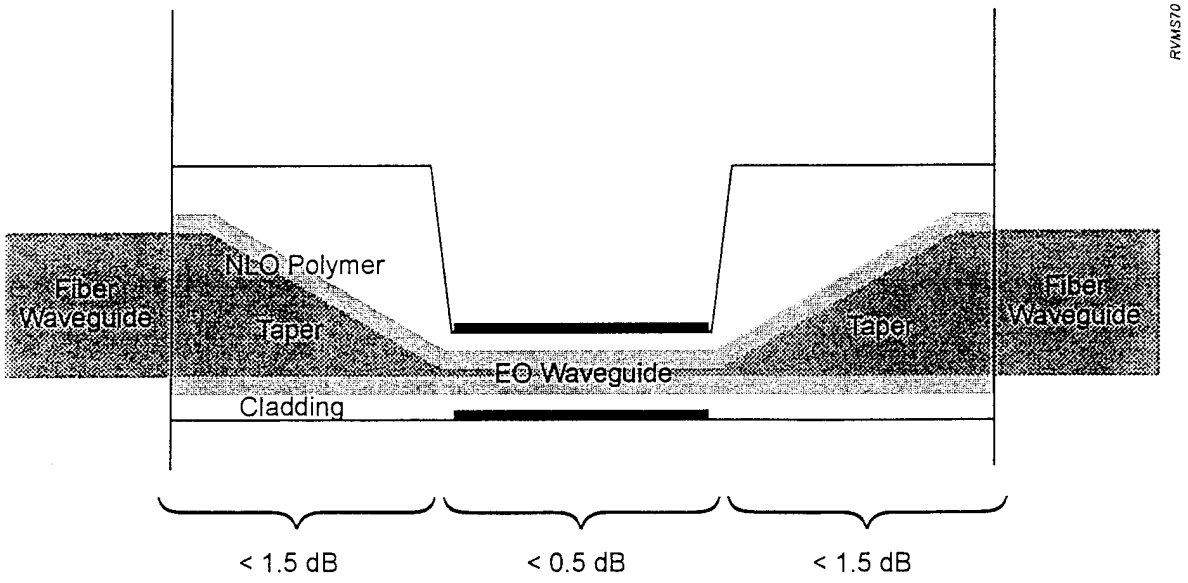

Figure 27. Fabrication of tapered transitions from fiber to small waveguide in an NLO polymer device.

The above described vertical taper can then smoothly transition the waveguide to a waveguide of small vertical dimension. Such a waveguide does not necessarily need to laterally narrow as illustrated by the flattened mode shape shown in Figure 27. This may or may not be required depending upon device's electrode requirements.

Theoretical analyses of dielectric waveguide tapers suggest that virtually loss less tapers can be made following certain optimum profiles. Such a contour is shown in Figure 28 following the calculations of Marcatili (Sakai and Marcatili, 1991). The prescribed functional form of this loss less dielectric taper is

$$n(r,\theta,\psi) = n_0\sqrt{1+\left(\frac{a\sqrt{2\Delta}}{r}\right)^2\left(D_1^2 \pm D_2^2 \sin^2\theta\right)} \qquad for\ \theta_1 \le \theta \le \theta_2$$

where the index n is in spherical coordinates, n_0 is the cladding index, Δ is the relative index difference between core and cladding, and the D parameters relate mode index to angle. Figure 28 shows that the wider the taper width is, the lower the refractive index is in order to maintain a constant mode support along the r axis during propagation in a loss less taper. To simplify illustrations of tapers, all tapers have been depicted as linear, but note that the optimum taper profiles have a more complicated nonlinear profile. Allowing for intrinsic polymer optical loss and fabrication imperfections, a loss of 0.5 dB for a taper transition should be feasible through photoprocessing and the use of these optimum transition profiles. As illustrated in Figure 27, this suggests a total insertion loss of <3.5 dB for an approximately 1 inch waveguide having entrance and exit tapers to fiber and a 10 mm length of NLO waveguide within a small electrode gap. A strong need for such a device architecture has been stated by Air Force researchers, but a practical fabrication approach has not been previously available.

4.3 REDUCED DRIVE VOLTAGE DESIGN FOR DEVICES

The ability to achieve a low loss transition to small device dimensions as illustrated in the previous section suggest that low drive voltages should be achievable using the EO coefficients available with current state-of-the-art NLO polymers. Large vertical Δn gradients created by the shorter wavelength photoprocessing serve effectively as cladding layers. The principal source of optical loss with closely spaced electrodes is usually the direct absorption of

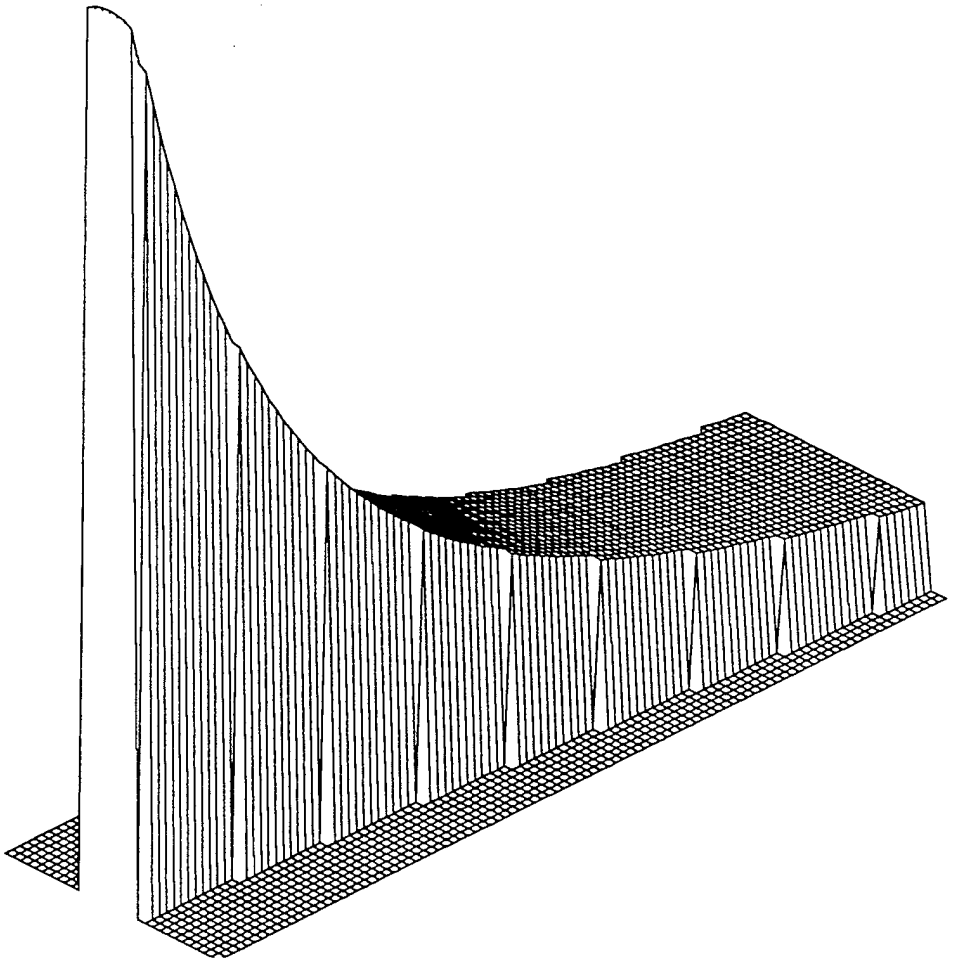

Figure 28. Theoretical profile for a loss less dielectric waveguide taper according to Marcatili (Sakai and Marcatili, 1991).

evanescent guided light in the cladding by the electrodes. Control of this large Δn gradient can be used to minimize the cladding thickness as well as the mode height in the waveguiding region.

The optical loss, α, due to electrode absorption can be expressed as (Reisinger, 1973; Kaminow et al., 1974)

$$\alpha = \frac{-\ln(T)}{2L_3 \tan \theta_3}$$

where the waveguide transmission T is

$$T = \Gamma_1 \Gamma_2 e^{-2\gamma_{3x} L_3}$$

and L_3 is the thickness of the guiding layer, θ_3 is the mode angle, Γ_i are the complex reflection coefficients, and γ_{3x} is the component of the complex wavenumber normal to the film surface. By solving for the complex propagation constant for the guided mode in this multi layer dielectric with complex indices (indices are complex for the metal electrodes), the imaginary part of the propagation constant can be determined. This approach is based upon published models for absorption loss in lossy dielectrics and has been previously tested with numerous experimental measurements of both slab and channel waveguide loss measurements of NLO polymers having varying thicknesses of cladding and metallization (Mustacich et al., 1992). Example calculation are shown in Figure 29 for PUDR19 layers of different thickness (2-4 μm) cladded symmetrically with different thickness claddings (horizontal axis) and coated with aluminum. Cladding thicknesses of approximately 1 μm are shown to contribute minimally to the optical propagation loss, even for very small waveguide dimensions of 2 μm.

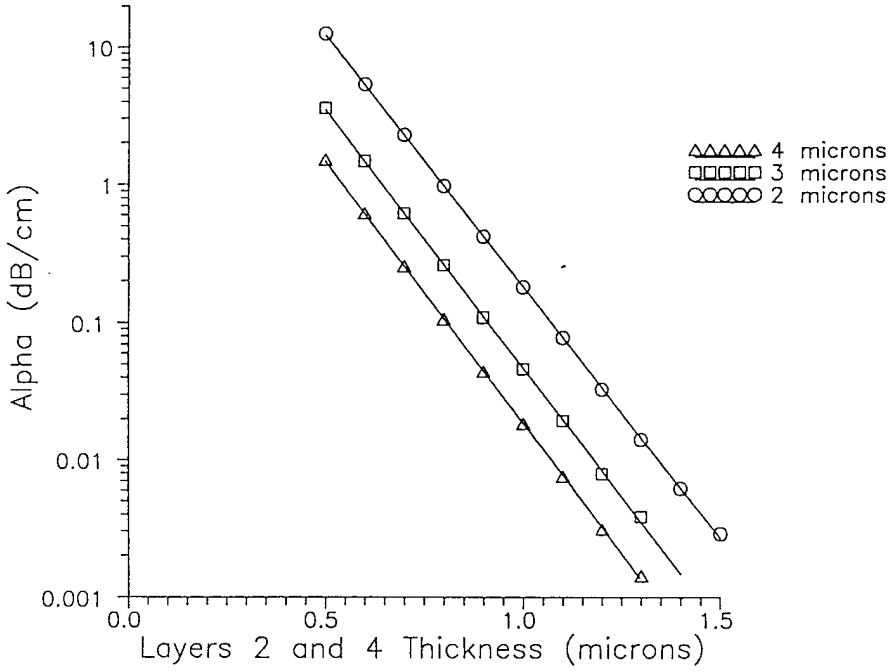

Figure 29. Calculated optical loss due to electrode absorption for thin claddings.

These calculations and photoprocessing results suggest that an approach such as dielectric etching can be used to remove excess cladding above the waveguide past the taper. Deposition of a metal electrode film above this etched region then provides a narrow electrode spacing. Sufficient NLO film thickness is left above the waveguide so that the absorption losses are minimized as required according to the calculations illustrated in Figure 29. The recommended sequence of the fabrication steps is summarized in Figure 30. This fabrication approach requires few steps and can provide high optical quality (low loss) waveguides with low cost fabrication.

1. Metal deposition
2. Cladding deposition
3. NLO polymer deposition
4. Multicolor photoprocessing
5. Dielectric etching
6. Metal deposition

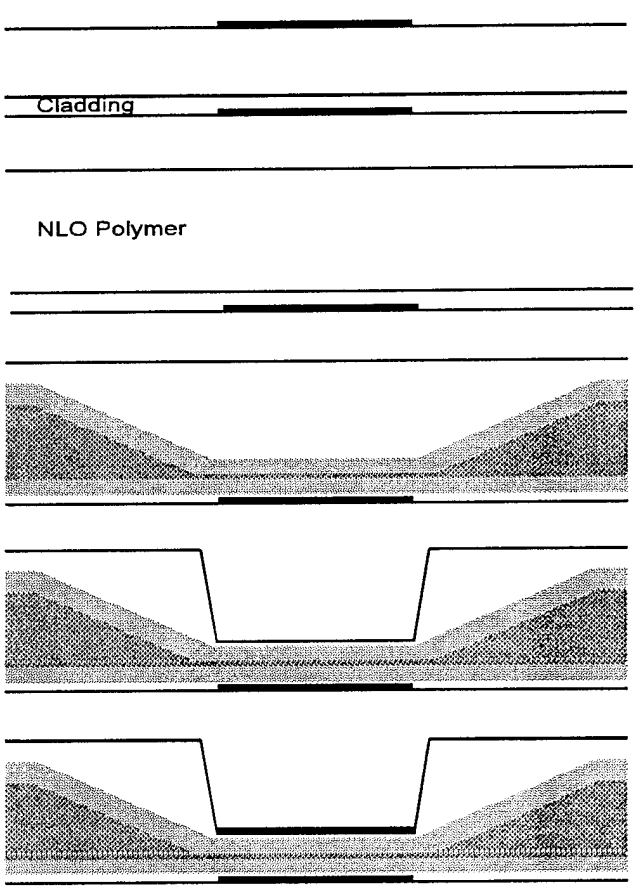

Figure 30. Sequence of processing steps for multicolor lithography of NLO polymer waveguide design for low insertion loss and small drive voltages.

5.0 REFERENCES

Born, M. and E. Wolf, Principles of Optics, Sixth Edition, Pergamon Press, New York, 1980, p. 575.

Caracci, S., "Second Order NLO Polymer Processing and Characterization at WPAFB," Air Force Nonlinear Optical Polymers Contractors Review Meeting, Fairborn, OH, February 26-28, 1996.

Chen, M., L. Yu, L. R. Dalton, Y. Shi and W. H. Steier, "New Polymers with Large and Stable Second-Order Nonlinear Optical Effects," Macromol. 24: 5421-5428, 1991.

Dill, F. H., W. P. Hornberger, P. S. Hauge and J. M. Shaw, "Characterization of Positive Photoresist," IEEE Trans. Electr. Dev. ED-22: 445-452, 1975.

Grote, J. "Optoelectronic Devices," Air Force Nonlinear Optical Polymers Contractors Review Meeting, Fairborn, OH, February 26-28, 1996.

Kaminow, I. P., W. L. Mammel, and H. P. Weber, "Metal-clad Optical Waveguides: Analytical and Experimental Study," Appl. Opt. 13: 396-405, 1974.

Mustacich, R., M. Gilbert, R. Finn and C. Swann, "Analysis and fabrication of overlapping-electrode designs for poling and modulating channels in polymer thin films," Appl. Opt. 31: 2800-2806, 1992.

Reisinger, A., "Characteristics of Optical Guided Modes in Lossy Waveguides," Appl. Opt. 12: 1015-1025, 1973.

Sakai, J. and A. J. Marcatili, "Lossless Dielectric Tapers with Three-Dimensional Geometry," J. Lightwave Technol. 9: 386-393, 1991.

Shi, Y., W. H. Steier, L. P. Yu, M. Chen and L. R. Dalton, "Large Induced Birefringence in an Optically Nonlinear Polyester Polymer," Appl. Phys. Lett. 2935-2937, 1991.

Shi, Y. "Fabrication and Testing High Speed Electro-Optic Polymer Modulators for Fiber-Optic Data Link Applications," Air Force Nonlinear Optical Polymers Contractors Review Meeting, Fairborn, OH, February 26-28, 1996.

Steier, W. H., Y. Shi, L. P. Yu, M. Chen and L. R. Dalton, Proc. SPIE 1775: 379, 1992.